[redacted]

#3

THE DAVID W. TAYLOR MODEL BASIN

UNITED STATES NAVY

OSCILLATION OF GAS GLOBES IN UNDERWATER EXPLOSIONS

BY ALFRED KEIL AND WALTER WUNDERLICH

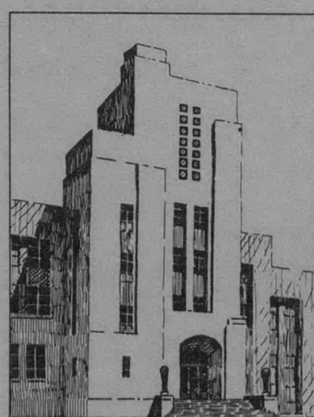

OCTOBER 1947

TRANSLATION 209

OSCILLATION OF GAS GLOBES IN UNDERWATER EXPLOSIONS

(DIE GASBLASENSCHWINGUNG BEI EINER UNTERWASSERSPRENGUNG)

by

Alfred Keil and Walter Wunderlich

Chemical-Physical Research Institute of the German Navy, Kiel, 1944
(Chemisch-Physikalische Versuchsanstalt der Marine, Kiel, 1944)

Translated by R. Widmer

Navy Department
David Taylor Model Basin
Washington, D.C.

October 1947 Translation 209

NOTATION

A, A_0	Capacity of gas globe for performing work or the energy of the gas globe
B	Work of displacement
c_r, C_r	Charge constants, see Equation [18]
c_T	$= C_T \eta_T$, impact-time constant
C_T	See Equation [22]
D	Velocity of detonation
e	See Equation [38]
E	Kinetic energy
E_{max}	Maximum kinetic energy
E_S	Thrust energy
H_μ, J_μ	Functions of μ, see Equation [20]
L	Weight of charge
m	$= \frac{r_{max}}{r_0}$, the expansion factor of gas globe from the initial state to the state of maximum expansion
p, p_0	Pressure in the gas globe
p_a	Hydrostatic pressure
P, Q	See Equation [25]
Q	Heat of reaction
r	Radius of gas globe
r_a	Radius of gas globe with internal pressure p_a
r_{max}	Maximum radius of gas globe
r_0	Charge radius
R	$= \frac{1}{\sqrt{Q}} - \Omega$
R	Gas constant
s	Radius of an imaginary hollow sphere surrounding a gas globe
S	Density of an explosive in kg/cm^3
s'	Density of an explosive in gm/cm^3
t	Time
T, T'	Period of oscillation
T_1	Sonic oscillation period
v	Specific quantity of gas
V, V_0	Volume of gas globe
x	$= r/r_0$
α	See Equation [7]
β	See Equation [7]
γ'	Density of liquid
μ	$= r_0/r_{max}$

η_r Correction factor, see Equation [15]

η_T Correction factor, see Equation [30]

ρ Specific mass of the liquid

κ Ratio of specific heats of gases, i.e., c_p/c_v

ϕ See page 17

Ω See page 19

τ Absolute temperature of a gas

τ_0 Initial temperature of a gas

TABLE OF CONTENTS

OSCILLATION OF GAS GLOBES IN UNDERWATER EXPLOSIONS

FOREWORD

Many attempts have been made to find suitable units of measurement for the correct evaluation of underwater explosions. It would lead entirely too far afield to outline the development of this problem in all its details; therefore, only the main points of the problem will be emphasized.

Until recently, for example, the velocity of detonation D and the specific quantity v_G of gas of the explosive were regarded as basic characteristics for the effect of underwater explosions, wherein the product v_GD was accorded special consideration. The German Navy, on the other hand, has long considered the energy content of the explosive, determined as the heat of reaction during the reaction in the calorimeter, far more essential to the effectiveness of underwater explosives. Aside from these pure measured values, some additional data on effectiveness were found, such as the expansion of lead blocks, i.e., the expansion produced by the explosion of a given quantity of explosive inside a lead block of given quality and shape, or earth displacement, i.e., the size of the crater produced in the ground by a given charge under certain given conditions. Both of these criteria are often used also for the characterization of the underwater effect of explosives.

The evaluation and analysis of these measured data on the effectiveness of explosives under water are not at all uniform. It is clear from the outset that lead-block expansion and earth displacement give only empirical values, since both these test methods are fundamentally based on unjustifiable or only partially justifiable analogies. The effect of the velocity of detonation and the specific quantity of gas on the underwater effect are likewise surmises based on certain assumptions. Neither, however, does the only energy value, i.e., the heat of reaction Q, determined by reaction of the explosive as measured in a calorimeter, correspond entirely to conditions underwater; as shown by tests, the gases expand more rapidly under water than in the calorimeter, and, moreover, portions of the gases react with the ambient water. It is obvious, therefore, that the methods mentioned in the foregoing as being in general use do not afford a reliable means of evaluating the effectiveness of explosives under water.

A suitable and logical index for underwater explosives can be found only by a systematic treatment of the physical phenomena which occur in underwater explosions. As experience has shown, neither a description nor an experimental investigation of these phenomena can supply such an index; only a clear, comprehensive, theoretical investigation of the problem can do so. A mathematical treatment which clearly describes the phenomena of underwater explosions by use of the most simplifying assumptions, and which at the same time gives their development with time in surprisingly good agreement with experimental data, is developed herein.

As will be shown, by thus avoiding the dilemma of test data, an easily determined index for each underwater explosive is attained. This index is the so-called gas globe energy. The particular value of this datum lies in the fact that by its use one of the effects of underwater explosions which is most essential for the sinking or damaging of ships is definitively characterized.

The general necessity and the practical importance of a correct theoretical treatment of the phenomena involved in underwater explosions having been brought out, the theory will now be presented.

1. BASIC ASSUMPTIONS

For every theoretical investigation of the problem of underwater explosions, a large number of basic assumptions is necessary. The more these assumptions are simplified, the easier the mathematical treatment becomes in general, but the less valuable are the results. In this case, a proper sense of values must be maintained. Therefore, the basic assumptions used must be such as to correctly typify the characteristics of the phenomenon while reducing mathematical difficulties to a minimum.

Before these assumptions for the mathematical treatment of this problem are established, the actual conditions in an underwater explosion at considerable depths will be briefly and clearly presented.

The gases formed in the total detonation of the explosive which proceeds at a velocity of 5000 to 8000 m/sec are subject to high pressure as they practically occupy the space originally taken by the explosive and also carry the energy released by the detonation. Therefore they represent an underwater gas globe which generally is not initially spherical, but which in the course of expansion rapidly becomes a nearly perfect sphere as photographs show; see Figure 1.

The water surrounding the gas globe is compressed and pushed back by the highly compressed gases. As a result of the compression of the water, a pressure wave propagates from the point of detonation while simultaneously the mass of water absorbs kinetic energy at the cost of the potential energy contained in the gases, with resulting pressure drop in the gas globe. The acceleration of the water is stopped until the pressure in the gas globe attains the external pressure which prevailed at the point of detonation before detonation. Whereas up to this stage, therefore, the surrounding water was pushed back by the gas globe, the globe is now distended further by the surge

Figure 1 - Gas Globe from 5-Gram Charge of TNT at Maximum Expansion
The inside diameter of the gas globe is 52 cm. The charge depth was 1 m.

of the water masses. This motion is retarded by the negative pressure now arising in the gas globe, until the motion of the water finally ceases and even reverses. The water masses now surge back toward the point of detonation, the pressure in the gas globe increasing steadily during the process. If there were no energy losses, the gas globe would necessarily revert to its initial state which prevailed after the total detonation of the explosive. However, this is not the case as, owing to compressibility of the water, a pressure wave was propagated at the very beginning and a new pressure wave results from the insurge of the water. In addition, further energy losses result from thermal conduction, viscosity, and so on. Therefore, the contracting gas globe does not quite reach its initial state but does reach a minimum at which the gases are again highly compressed so that they must once again expand. The phenomenon of oscillation of the gas globe just described therefore repeats itself in a similar way. Thus a number of constantly damped oscillations and various pressure waves, briefly termed "impacts," result; see Figure 2.

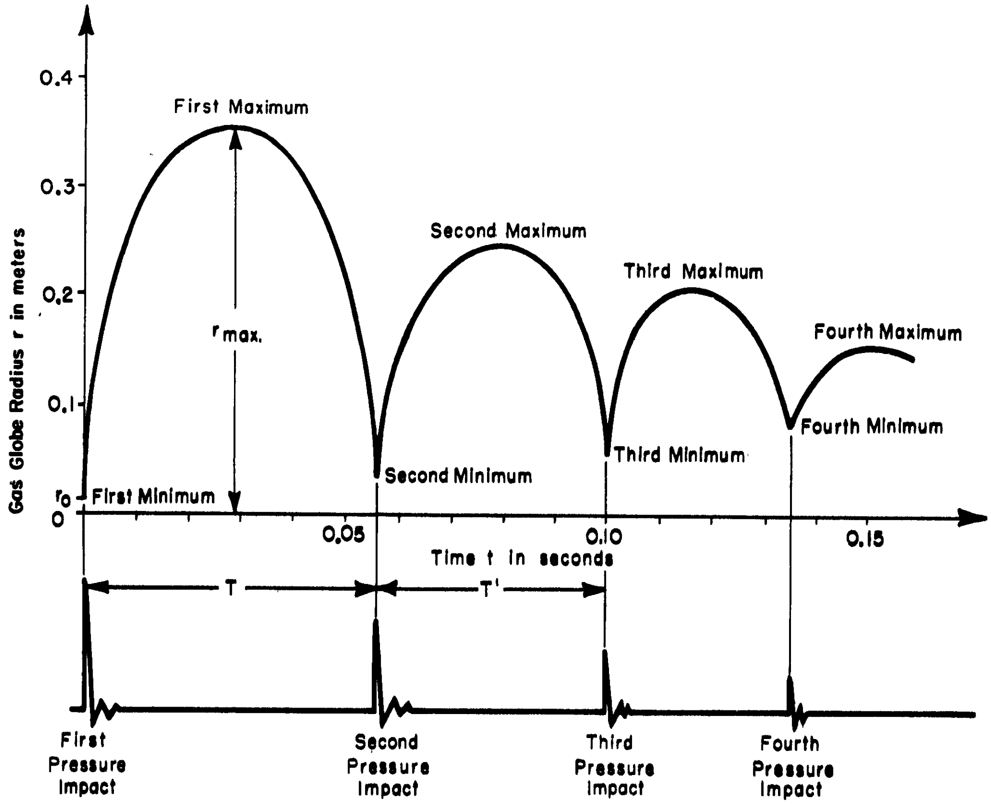

Figure 2 - Schematic Diagram of Gas Globe Oscillation and Radiation of Pressure Impacts

Following this broad description of the phenomena in an underwater explosion, the basic assumptions for the theoretical treatment of the problem can be set up. A stationary, infinite, incompressible liquid is assumed. In this liquid, at a point where the hydrostatic pressure p_a prevails, let there be a spherical gas globe whose volume is V_0 and in which the pressure $p_0 > p_a$. Owing to positive pressure, the gas globe begins to expand, retaining its spherical shape. If the buoyancy is disregarded, the flow of the liquid being displaced is then purely radial. Therefore, it is assumed in the following that before detonation a uniform pressure p_a prevails everywhere in the liquid. The content of the gas globe is assumed to be an ideal gas whose change of state proceeds adiabatically. The curve of motion of the front of the gas, determined by this assumption, is to be investigated.

These assumptions naturally represent considerable simplifications. Even if the gas globe is almost perfectly spherical and the water surrounding the charge before the first oscillation can be considered stationary, the water actually is neither of infinite extent nor incompressible. However, as the displacement flow at a greater distance from the point of explosion is very small, being inversely proportional to the square of the distance, the assumption of infinite extent of the liquid is practically satisfied at sufficient charge depth. The pressure drop as a function of gravity over the gas globe imparts buoyancy to it and causes it to rise to the surface. This effect cannot be considered at the moment but is, as experience has shown, of secondary importance for small charges up to 1 kg. The compressibility of the water is small in itself but plays a part which cannot be disregarded at the high explosive pressures which occur at the beginning of the motion and in the vicinity of the minima. A considerable amount of energy is therefore expended as a pressure wave. However, once the pressure wave is released, which takes place within a very short time as the internal pressure of the gas globe drops rapidly, the remaining and preponderant part of the oscillation occurs as in an incompressible liquid. By treating the composite mixture of the products of combustion as an ideal gas, van der Waals' forces are neglected, although they should very probably be considered because of the high compression at the start. The assumption that the change of state is adiabatic can be considered as justified in view of the poor thermal conduction and the velocity of the oscillation. Otherwise, the problem of a thermal exchange in both directions would arise, as the products of combustion are initially very hot but soon cool to far below the temperature of the surroundings. A special place is occupied by explosive mixtures containing aluminum. With these it must be assumed that the products of combustion undergo a secondary reaction which produces an additional output of energy during the oscillation of the gas globe.

In summarizing, it can be expected that the investigation of oscillation of gas globes under the conditions mentioned in the beginning will at least describe well the first oscillation for underwater detonation at sufficient charge depth.

Naturally, it is possible to simplify the basic assumptions even more. H. Lamb (1),* for example, treated the problem with the foregoing basic assumptions neglecting in addition only the pressure p_a; i.e., he assumed $p_a = 0$. However, the most essential part of the expansion of the products of combustion, namely the course of the oscillation, is lost. M. Minnaert (2) on the other hand, on the basis of the foregoing assumptions, postulated the pressure fluctuations as very small with respect to external pressure ($p_0 - p_a << p_a$). He thus obtained the "sonic" oscillation of gas globes. With these additional simplifications, the oscillation of gas globes occurring in underwater explosions cannot be obtained.

On the other hand, less limiting basic assumptions can naturally be chosen. If, in contrast to the foregoing assumptions, the water is assumed

* Numbers in parentheses indicate references on page 50 of this translation.

as not absolutely incompressible but compressible, as was done by Zoller (3), Döring (4), and Gerhartz (5), the pressure wave and damping of the gas globe oscillation are found theoretically, but the problem can no longer be solved generally but only approximately and numerically. Moreover the actual conditions, especially those pertaining to the pressure wave, are not approached either since the pressure wave would have to be treated as a shock wave of variable velocity, because of its high amplitude.

It will be shown that precisely with the aforementioned basic assumptions an accurate, complete integration of the equation for motion of the phenomenon is possible without undue mathematical difficulties; moreover, it will be shown also that the individual oscillation is reproduced by this theory with astonishing exactitude and that quite definitive applications of this theory are possible.

The investigations herein described were made some time ago by the CPVA.* Shortly thereafter, a treatment of the same problem for incompressible water was published by Zoller (6) which, however, was not as extensive. The results obtained are summarized here once more because the impression might arise that, owing to the numerous investigations of the problem of detonation under water which have appeared meanwhile, treatment of this problem on the assumption of incompressible water is no longer important.

2. BASIC THEOREM

The clearest and simplest approach to the mathematical treatment of the motion of gas globes can be made by establishing the balance of energy, as done by C. Ramsauer (7). If the gas globe has expanded from the condition of p_0, V_0 to the condition p,V its capacity for performing work (internal energy) has decreased from

$$A_0 = \frac{p_0 V_0}{\kappa - 1} \text{ to } A = \frac{pV}{\kappa - 1} \qquad [1]$$

where p is measured in atmospheres or kilograms per centimeter^2, V in centimeters^3, and A in kilogram-centimeters. Therefore, A_0 will always be designated as the energy of the gas globe in this report. Moreover, $\kappa = c_p/c_v$ is the (constant) ratio of the specific heats of the gas. The value of κ can be assumed to lie in the range from 1.2 to 1.4. As the change of state occurs adiabatically and is controlled by Poisson's law

$$pV^\kappa = \text{constant} = p_0 V_0^{\,\kappa} \qquad [2]$$

the difference $A_0 - A$ has been converted merely into mechanical work. The

---

* Translator's Note: CPVA signifies "Chemisch-Physikalische Versuchsanstalt der Marine" (Chemical-Physical Research Institute of the German Navy).

latter consists of two types: First, the external pressure p_a, which is constant by assumption, was overcome over the surface of a sphere of volume $V - V_0$, which corresponds to the work performed of

$$B = p_a(V - V_0) \qquad [3]$$

Second, kinetic energy E was imparted to the surrounding water. To compute E, the surrounding medium will be assumed as divided into a series of hollow spheres. If the radius r of the gas globe increases by dr, the radius of the hollow sphere s simultaneously changes by ds. From the equality of the displaced quantities of liquid (continuity in incompressible media) it follows first that

$$4\pi r^2\, dr = 4\pi s^2\, ds$$

and, dividing by the time differential dt for the velocities $\dot{r} = dr/dt$ and $\dot{s} = ds/dt$

$$\dot{s} : \dot{r} = r^2 : s^2 \qquad [4]$$

The local decrease of the velocity of flow $\dot{s}$ at a given time t is therefore found to be inversely proportional to the square of the distance s from the point of detonation.

If the specific mass of the liquid is designated by ρ, where ρ is in kilogram-seconds^2 per centimeter^4, the portion of the kinetic energy imparted to the hollow sphere with a radius of s and a thickness of ds is

$$dE = 2\pi\rho s^2\, ds\, \dot{s}^2 = 2\pi\rho r^4 \dot{r}^2 \frac{ds}{s^2}$$

By integration from the edge of the globe to infinity, the total kinetic energy is found to be

$$E = 2\pi\rho r^4 \dot{r}^2 \int_r^\infty \frac{ds}{s^2} = 2\pi\rho r^3 \dot{r}^2 \qquad [5]$$

If, in Equations [1], [2], and [3], the spherical volume V or V_0 is expressed in terms of the radius r or r_0, the equation for energy

$$A_0 - A = B + E$$

leads to the differential equation of the oscillation of gas globes

$$\frac{3\rho}{2}\dot{r}^2 = \frac{p_0}{\kappa - 1}\left[\left(\frac{r_0}{r}\right)^3 - \left(\frac{r_0}{r}\right)^{3\kappa}\right] + p_a\left[\left(\frac{r_0}{r}\right)^3 - 1\right] \qquad [6]$$

The introduction of the nondimensional coordinate $x = r/r_0$ (gas globe radii in "charge radii") is obvious:

$$\underbrace{\frac{3(\kappa - 1)\rho r_0^2}{2p_0}}_{\beta^2} \cdot \dot{x}^2 = \frac{1}{x^3} - \frac{1}{x^{3\kappa}} + \underbrace{\frac{(\kappa - 1)p_a}{p_0}}_{\alpha^3}\left(\frac{1}{x^3} - 1\right)$$

By use of the abbreviations

$$\alpha = \sqrt[3]{\frac{(\kappa - 1)p_a}{p_0}} \text{ and } \beta = r_0\sqrt[2]{\frac{3(\kappa - 1)\rho}{2p_0}} \tag{7}$$

the differential equation becomes

$$\beta\dot{x} = \frac{1}{x^2}\sqrt{x - x^{4-3\kappa} + \alpha^3(x - x^4)} \tag{8}$$

It can then be solved directly by squaring:

$$t = \beta\int_1^x \frac{x^2\,dx}{\sqrt{x - x^{4-3\kappa} + \alpha^3(x - x^4)}} \tag{9}$$

An elementary evaluation of the integral is not possible.

3. MAXIMUM GLOBE RADIUS

The maximum state of expansion of the gas globe is connected with a reversal of motion and therefore is characterized by vanishing velocity, $\dot{r} = 0$. For the determination of the corresponding globe radius r_{max}, Equation [6] whose left side is set equal to zero therefore suffices. If we introduce

$$\frac{r_0}{r_{max}} = \mu \tag{10}$$

the equation

$$\mu^3 - \mu^{3\kappa} + \alpha^3(\mu^3 - 1) = 0 \tag{11}$$

will have to be solved. The reciprocal of μ

$$m = \frac{1}{\mu} = \frac{r_{max}}{r_0} = x_{max} \tag{12}$$

will be called the "expansion factor" and is important for clarity: m represents the linear expansion factor of the gas globe from the initial state to the state of maximum expansion. For the first oscillation of the gas globe in underwater explosions, m is approximately of the order of 30; μ is hence small. Under these conditions, $\mu \approx \alpha$ in the first approximation, as can be recognized by restating Equation [11] as

$$\alpha^3 = \mu^3 \frac{1 - \mu^{3\kappa-3}}{1 - \mu^3} \approx \mu^3 \qquad [13]$$

It is therefore advisable to determine the particular correction factor η_r to be applied to α to get μ. From the condition that

$$\mu = \eta_r \alpha = \eta_r \sqrt[3]{\frac{(\kappa - 1)p_a}{p_0}} \qquad [14]$$

it follows that

$$\eta_r = \sqrt[3]{\frac{1 - \mu^3}{1 - \mu^{3\kappa-3}}} \; ; \; \alpha = \frac{\mu}{\eta_r} \qquad [15]$$

Thus η_r and α appear as functions of the parameter μ. If μ is carried through from 0 to 1 and if values of η_r and α which belong together are plotted on rectangular coordinates, a curve is obtained which permits reading the correction η_r for each value of α. Figure 3 gives these curves for $\kappa = 1.2$, 1.3, 4/3, and 1.4. From these and with Equations [10] and [14], determination of the maximum radius of the globe is possible with satisfactory accuracy, as

$$r_{\max} = \frac{r_0}{\mu} = \frac{r_0}{\eta_r \alpha} = \frac{r_0}{\eta_r} \sqrt[3]{\frac{p_0}{(\kappa - 1)p_a}} \qquad [16]$$

If the charge radius r_0 is expressed in terms of the weight of the charge L and the density of the explosive s to which it is related by

$$L = \frac{4\pi}{3} r_0{}^3 s \;\text{ or }\; r_0 = \sqrt[3]{\frac{3L}{4\pi s}} \qquad [17]$$

where L is in kilograms and s is in kilograms per centimeter^3, we find that

$$r_{\max} = c_r \sqrt[3]{\frac{L}{p_a}} \;\text{ with }\; c_r = \frac{C_r}{\eta_r} \;\text{ and }\; C_r = \sqrt[3]{\frac{3p_a}{4\pi(\kappa - 1)s}} \qquad [18]$$

This is the familiar formula for the radius of the gas globe (7). The "constant" c_r is to some extent also a function of the external pressure p_a, contained in the correction factor η_r. The true charge constant is C_r; for TNT it is about 160 (in the German system of units). The effect of the correction factor η_r increases with the depth because α and therefore η_r increase with p_a. However, the difference amounts to only a few per cent, as can be seen in Figure 3.

It should be emphasized that the maximum radius of the globe is not a function of the surrounding liquid, as could be concluded by the disappearance of the single term containing ρ in Equation [6].

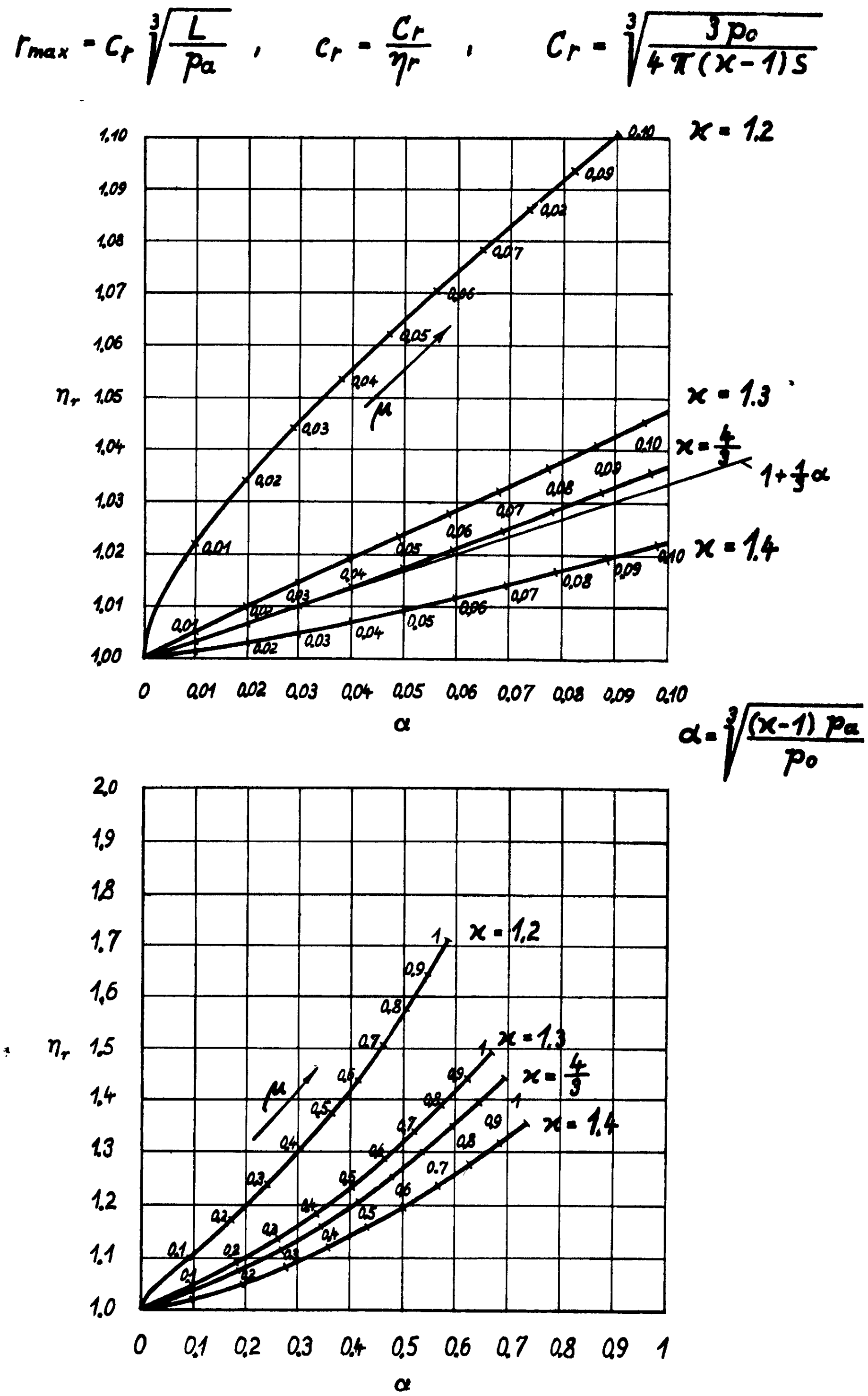

Figure 3 - Correction Factor η_r

The particular case where $\kappa = 4/3$ deserves special mention; here the fraction under the radical sign in Equation [15] can be reduced by $1 - \mu$, giving

$$\eta_r = \sqrt[3]{1 + \mu + \mu^2} = 1 + \frac{1}{3}\mu + \frac{2}{9}\mu^2 - \cdots$$
$$\alpha = \frac{\mu}{\eta_r} = \mu - \frac{1}{3}\mu^2 - \frac{1}{9}\mu^3 + \cdots \qquad [15']$$

and by inversion

$$\mu = \alpha + \frac{1}{3}\alpha^2 + \frac{1}{3}\alpha^3 + \cdots; \quad \eta_r = 1 + \frac{1}{3}\alpha + \frac{1}{3}\alpha^2 + \cdots$$

The terms set down in the development of the exponential series are entirely sufficient over the principal range involved where $0 \leqq \alpha \leqq 0.1$. The reciprocal $1/\eta_r$ appearing in Equation [18] starts with $1 - \frac{1}{3}\alpha$.

Generally κ can only be computed by a development with fractional exponents; therefore this development is not very valuable, that is

$$\eta_r = 1 + \frac{1}{3}\mu^{3\kappa-3} + \frac{2}{9}\mu^{6\kappa-6} + \cdots; \quad \eta_r = 1 + \frac{1}{3}\mu^{3\kappa-3} + \frac{3\kappa - 1}{9}\alpha^{6\kappa-6} + \cdots$$

4. PERIOD OF THE OSCILLATION (FIRST APPROXIMATION)

To calculate the period of the oscillation T, the integral of Equation [9] must be extended to the upper limit $x_{max} = m$ and doubled. It is recommended, therefore, to introduce the variable of integration

$$y = \mu x = \frac{r}{r_{max}}$$

Then

$$T = \frac{2\beta}{\mu}\int_{\mu}^{1}\frac{y^2\,dy}{\sqrt{\mu^3 y - \mu^{3\kappa}y^{4-3\kappa} + \alpha^3(\mu^3 y - y^4)}}$$

If α^3 is also expressed in terms of the parameter μ according to Equation [13], μ^3 can be removed from under the radical sign, so that

$$T = \frac{2\beta}{\mu^{5/2}}\int_{\mu}^{1}\frac{y^2\,dy}{\sqrt{y - \mu^{3\kappa-3}y^{4-3\kappa} + \dfrac{1-\mu^{3\kappa-3}}{1-\mu^3}(\mu^3 y - y^4)}} \qquad [19]$$

The integral is a function of the parameter μ and therefore will be designated hereafter by J_μ. As the value $\mu = r_0/r_{max}$ for the first oscillation of the gas globe in underwater explosions is small, that is, $\mu \approx 1/30$, a first approximation is obtained by setting $\mu = 0$, as follows:

$$J_\mu \approx J_0 = \int_0^1 \frac{y^2\,dy}{\sqrt{y - y^4}} = \int_0^1 \sqrt{\frac{y^3}{1 - y^3}}\,dy \qquad [20]$$

By substituting $y^3 = u$, J_0 can be traced to Euler's β-function and can be expressed by Γ-functions as

$$J_0 = \frac{1}{3}\int_0^1 u^{-1/6}(1-u)^{-1/2}du = \frac{1}{3}B\left(\frac{5}{6},\frac{1}{2}\right) = \frac{1}{3}\,\frac{\Gamma\left(\frac{5}{6}\right)\Gamma\left(\frac{1}{2}\right)}{\Gamma\left(\frac{4}{3}\right)}$$

$$= \frac{\sqrt{\pi^3}}{9\Gamma\left(\frac{4}{3}\right)\Gamma\left(\frac{7}{6}\right)} = \frac{2\sqrt[3]{2}}{\sqrt{3}}\,\frac{\pi^2}{\Gamma^3\left(\frac{1}{3}\right)} = 0.74683 \qquad [21]$$

Therefore, in the first approximation, with consideration for Equations [7] and [17],

$$T \approx \frac{2J_0\,\beta}{\mu^{5/2}} \approx \frac{2J_0\,\beta}{\alpha^{5/2}} = 2J_0\sqrt[3]{\frac{3L}{4\pi s}}\sqrt[2]{\frac{3(\kappa-1)\rho}{2p_0}}\sqrt[6]{\frac{p_0{}^5}{(\kappa-1)^5 p_a{}^5}}$$

If the density s' of the charge and the density γ' of the liquid, expressed in the usual unit, grams per centimeter^3, are substituted in the collection of the radicals, the result is $s = s'/1000$, $\rho = \gamma'/981{,}000$, and, written as usual,

$$T \approx C_T\sqrt[3]{\frac{L}{p_a{}^{2.5}}}\sqrt{\gamma'} \text{ with } C_T = \frac{0.03J_0}{\sqrt[6]{6}\,\sqrt[3]{\pi}\,\sqrt{0.981}}\sqrt[3]{\frac{p_0}{(\kappa-1)s'}} \qquad [22]$$

The excellence of this approximation becomes clearly apparent in the following section.

5. PERIOD OF THE OSCILLATION (SECOND AND THIRD APPROXIMATIONS FOR $\kappa = 4/3$)

To get a closer estimate of the oscillation period T, the integral J_μ in Equation [19] will be conceived as developed in a potential series with respect to μ. As only a progressive development by exponents which are whole numbers is of interest, only the special case $\kappa = 4/3$ will be considered from the outset. Then the fraction under the radical sign can be reduced by $1 - \mu$ and we have

$$T = \frac{2\beta\sqrt{1+\mu+\mu^2}}{\mu^{5/2}}\int_\mu^1 \frac{y^2\,dy}{\sqrt{(1+\mu+\mu^2)(y-\mu) - y(y^3-\mu^3)}} \qquad [23]$$

The integral, which will be designated by H_μ, must be treated with some caution, as it is singular, the radicand in the denominator vanishing at both limits. For this reason, the two root factors $(y - \mu)$ and $(1 - y)$ are first split off and we have

$$H_\mu = \int_\mu^1 \frac{y^2\,dy}{\sqrt{(y-\mu)(1-y)}\,\sqrt{y^2+(1+\mu)y+(1+\mu+\mu^2)}} \qquad [24]$$

The second root hence no longer possesses any null points over the interval of integration and therefore represents a regular component of the integral. To establish fixed limits, the integral is transformed by $y = z + \mu(1 - z)$ and thus we get

$$H_\mu = \int_0^1 \frac{P\,dz}{\sqrt{z(1-z)}\,\sqrt{Q}}$$

with

$$P = \underbrace{z^2}_{P_0} + \mu\underbrace{2z(1-z)}_{P_0'} + \mu^2\underbrace{(1-z)^2}_{\frac{1}{2}P_0''} \qquad [25]$$

and

$$Q = \underbrace{(1+z+z^2)}_{Q_0} + \mu\underbrace{2(1+z-z^2)}_{Q_0'} + \mu^2\underbrace{(3-3z+z^2)}_{\frac{1}{2}Q_0''}$$

The expression $Z = P/\sqrt{Q}$ is a regular function for all values of z in $\mu = 0$, and can therefore be developed in an exponential series.

$$Z = PQ^{-1/2} = Z_0 + \mu Z_0' + \frac{\mu^2}{2}Z_0'' + \cdots$$

with $Z_0 = P_0 Q_0^{-1/2}$

$$Z_0' = (PQ^{-1/2})_0' = P_0' Q_0^{-1/2} - \frac{1}{2}P_0 Q_0' Q_0^{-3/2} \qquad [26]$$

$$Z_0'' = (PQ^{-1/2})_0'' = P_0'' Q_0^{-1/2} - P_0' Q_0' Q_0^{-3/2} - \frac{1}{2}P_0 Q_0'' Q_0^{-3/2} + \frac{3}{4}P_0 Q_0'^2 Q_0^{-5/2}$$

The values of P_0, Q_0, etc., are found by Equation [25]; substituting them gives

$$\frac{P}{Q} = \frac{z^2}{\sqrt{1+z+z^2}} + \mu\frac{z(2-z-z^2-z^3)}{\sqrt{(1+z+z^2)^3}} + \mu^2\frac{1-2z-2z^2+3z^3}{\sqrt{(1+z+z^2)^5}} + \cdots \qquad [27]$$

Then dividing by $\sqrt{z(1-z)}$ according to Equation [25] and integrating by terms from 0 to 1 (all integrals appearing are singular but do exist) the desired development

$$H_\mu = H_0 + \mu H_0' + \frac{\mu^2}{2} H_0'' + \cdots$$

is found. As it must be, H_0 is identical with J_0 and therefore can be taken from Equation [21]. By letting $z^3 = u$, the remaining integrals can be related also to Γ-functions

$$H_0' = \int_0^1 \frac{(2 - z - z^2 - z^3)\sqrt{z}\,dz}{(1 + z + z^2)\sqrt{1 - z^3}} = 2\int_0^1 \frac{\sqrt{z} - \sqrt{z^3}}{\sqrt{(1 - z^3)^3}}\,dz - \int_0^1 \sqrt{\frac{z^3}{1 - z^3}}\,dz$$

$$= \frac{2}{3}\int_0^1 (u^{-1/2} - u^{-1/6})(1 - u)^{-3/2}\,du - J_0$$

$$= \frac{2}{3}\underbrace{B\left(\frac{1}{2}, -\frac{1}{2}\right)}_{0} - \frac{2}{3}B\left(\frac{5}{6}, -\frac{1}{2}\right) - J_0 = \frac{1}{3}J_0$$

The justification of the formal division into two nonexistent uniform integrals should be proved first, but this problem will not be taken up. Similarly, it is found that

$$H_0'' = \frac{4}{9}J_0 + \frac{4\pi\sqrt{3}}{27\,J_0}$$

Consequently,

$$H_\mu = J_0\left\{1 + \frac{1}{3}\mu + \left(\frac{2}{9} + \frac{2\pi\sqrt{3}}{27J_0^2}\right)\mu^2 - \cdots\right\} \qquad [28]$$

is found provisionally. Considering Equation [14] or respectively [15'], the factor directly preceding the integral in Equation [23] gives

$$\frac{2\beta\sqrt{1 + \mu + \mu^2}}{\alpha^{5/2}(1 + \mu + \mu^2)^{5/6}} = \frac{2\beta}{\alpha^{5/2}}(1 + \mu + \mu^2)^{-1/3} = \frac{2\beta}{\alpha^{5/2}}(1 - \frac{1}{3}\mu - \frac{1}{9}\mu^2 - \cdots)$$

The linear terms cancel after combination with H_μ from Equation [27] and there remains

$$T = \frac{2J_0\,\beta}{\alpha^{5/2}}\left(1 + \frac{2\pi\sqrt{3}}{27J_0^2}\mu^2 - + \cdots\right) \qquad [29]$$

Here, on the basis of Equation [15'], α can be substituted for μ and in comparison with Equation [22], it can be established that the right side of the formula for the period of the oscillation of the gas globe must be provided with a correction factor η_T whose initial development has just been outlined.

$$T = C_T \eta_T \sqrt[3]{\frac{L}{p_a^{2.5}}} \sqrt{\gamma'} \text{ with } \eta_T = 1 + \underbrace{\frac{2\pi\sqrt{3}}{27J_0^2}}_{0.72267 \approx \frac{13}{18}} \alpha^2 - \cdots \qquad [30]$$

For the definition of C_T see Equation [22].

The contribution of η_T for small values of α is but slight, as the linear term is lacking. The approximation, Equation [22], is therefore better than was to be expected, as it simultaneously represents the second approximation, at least for $\kappa = 4/3$. The agreement with the actual curve for η_T, as determined in the following section, is shown in Figure 4. A satisfactory approximation over the entire range from $0 \leqq \alpha \leqq 0.1$, which is the interval of principal interest, is attained by means of $\eta_T \approx 1 + \frac{2}{3}\alpha^2$.

The increase of the impact-time constant $c_T = C_T\eta_T$ with the charge depth is therefore barely noticeable. Hence, if variations have been determined despite this, they cannot be explained thus but must be traced to surface and bottom effects.

6. COURSE OF THE OSCILLATION OF THE GAS GLOBE

Determination of the oscillation period is accomplished satisfactorily by Equations [22] and [30] for small values of α or μ. For larger values apparent at later oscillations of gas globes, already weakened by damping, these equations do not suffice. Moreover, nothing has been stated as yet respecting the course of the oscillation. Both of these omissions will now be rectified.

Beginning with the integral expression, Equation [29], whose upper limit will now remain indeterminate, the roots $y - \mu$ and $1 - y$ are extracted from the denominator in a manner similar to that used in Equation [24] and

$$t = \frac{\beta}{\mu^{5/2}} \int_{\mu}^{y} \frac{y^2\,dy}{\sqrt{(y-\mu)(1-y)}\,\sqrt{Q}} \qquad [31]$$

with

$$Q = \frac{(1-\mu^3)(y - y^{4-3\kappa}\mu^{3\kappa-3}) + (1-\mu^{3\kappa-3})(\mu^3 y - y^4)}{(1-\mu^3)(y-\mu)(1-y)}$$

The first square root in the denominator is represented graphically as a semicircle on page 17. This suggests the following trigonometric substitution, which eliminates the singular component:

$$T = c_T \sqrt[3]{\frac{L}{p_a^{2.5}}}\sqrt{\gamma'}\ , \quad c_T = C_T\,\eta_T\ , \quad C_T = 0.00114577\ \sqrt[3]{\frac{p_o}{(\varkappa-1)\,S}}$$

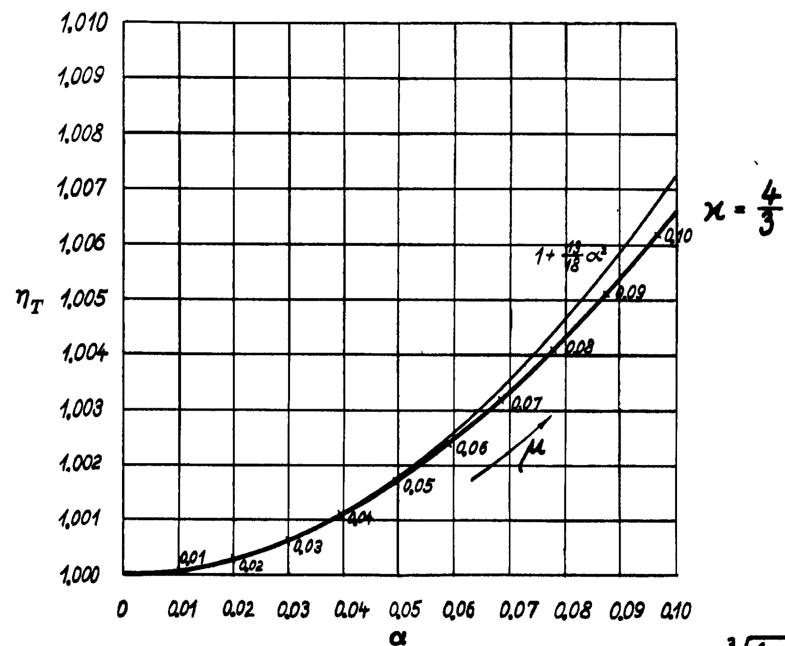

$$\alpha = \sqrt[3]{\frac{(\varkappa-1)\,p_a}{p_o}}$$

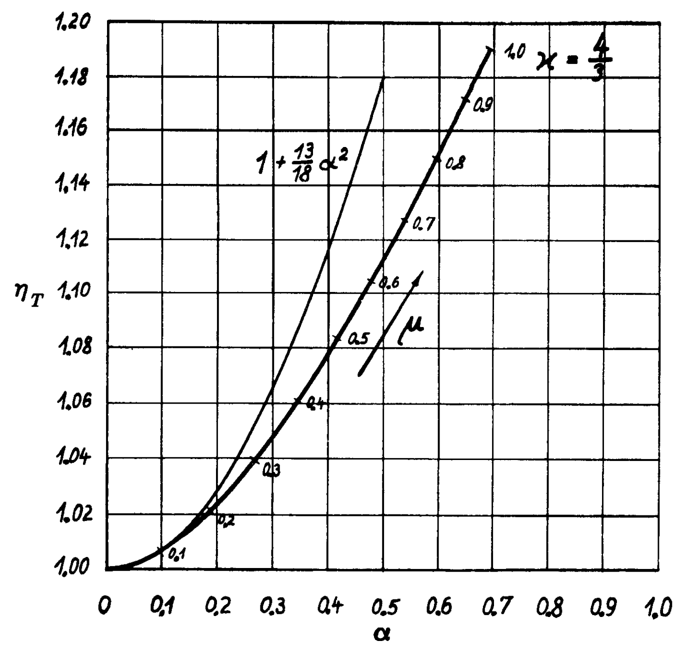

Figure 4 - Correction Factor η_T

$$y = \frac{1+\mu}{2} + \frac{1-\mu}{2}\cos\phi$$

$$dy = -\frac{1-\mu}{2}\sin\phi\, d\phi$$

$$\sqrt{(y-\mu)(1-y)} = \frac{1-\mu}{2}\sin\phi$$

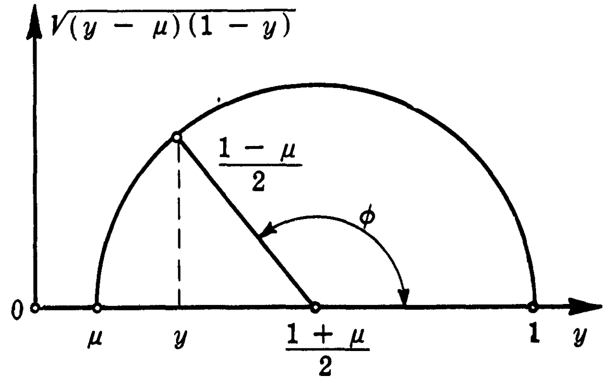

The remainder of the basic concept is devoted to the attempt to approximate the absolutely finite function $1/\sqrt{Q}$ by a cosine polynomial, that is, to undertake development of a type of Fourier series by which the integral can be evaluated with any desired accuracy. The rather extensive numerical computations required could be made only for the relatively simple case where $\kappa = 4/3$, due to shortage of time and because no calculating machine was available. Here Q can be simplified by the root factors and by $1 - \mu$ (compare Equation [24]) and it is found that

$$t = \frac{\beta}{\mu^{5/2}}\int_0^\phi \frac{P\,d\phi}{\sqrt{Q}}$$

with

$$P = y^2 = \frac{3 + 2\mu + 3\mu^2}{8} - \frac{1-\mu^2}{2}\cos\phi + \frac{(1-\mu)^2}{8}\cos 2\phi \qquad [32]$$

and

$$Q = \frac{y^2 + (1+\mu)y + (1+\mu+\mu^2)}{1+\mu+\mu^2}$$

$$= \frac{(15 + 18\mu + 15\mu^2) - 8(1-\mu^2)\cos\phi + (1-\mu^2)\cos 2\phi}{8(1+\mu+\mu^2)}$$

For reasons of symmetry, it suffices to extend the integration interval to $\phi = \pi$, corresponding to the globe maximum.

The course of calculation will be explained and illustrated with an important example where $\mu = 0$. The calculation procedure for any given value of μ is evident. For the functions P and $1 - \sqrt{Q}$, the values were calculated at 15-degree intervals; see Figure 5. The function P increases monotonically from $P(0) = \mu^2$ to $P(\pi) = 1$, whereas the function $1/\sqrt{Q}$ decreases monotonically The curves for both functions are horizontal at the beginning and at the end of the interval.

$$P_0 = \frac{3}{8} - \frac{1}{2}\cos\phi + \frac{1}{8}\cos 2\phi \qquad \frac{1}{\sqrt{Q_0}} = \Omega + R \approx \Omega$$

$$J_0 = \int_0^\phi \frac{P_0}{\sqrt{Q_0}}\, d\phi \qquad Q_0 = \frac{15}{8} - \cos\phi + \frac{1}{8}\cos 2\phi$$

$$\Omega = E + F\cos\phi + G\cos 2\phi \text{ with } \begin{cases} E = 0.771928 \\ F = 0.211325 \\ G = 0.016747 \end{cases}$$

ϕ degrees	P_0	$1/\sqrt{Q_0}$	Ω	R	$P_0\,R$	$\int P_0 \Omega\, d\phi$	$\int P_0 R\, d\phi$	J_0
0	0.00000	1.00000	1.00000	0.00000	0.000000	0.00000	0.00000	0.00000
15	0.00029	0.94145	0.99055	0.00090	0.000000	0.00002	0.00000	0.00002
30	0.00449	0.96608	0.96331	0.00277	0.000013	0.00046	0.00000	0.00046
45	0.02145	0.92534	0.92136	0.00398	0.000085	0.00328	0.00001	0.00329
60	0.06250	0.87288	0.86922	0.00366	0.000229	0.01251	0.00005	0.01256
75	0.13734	0.81435	0.81212	0.00223	0.000306	0.03377	0.00013	0.03390
90	0.25000	0.75593	0.75518	0.00075	0.000187	0.07265	0.00020	0.07285
105	0.39616	0.70262	0.70273	-0.00011	-0.000044	0.13370	0.00021	0.13391
120	0.56250	0.65758	0.65789	-0.00031	-0.000174	0.21822	0.00018	0.21840
135	0.72855	0.62231	0.62250	-0.00019	-0.000139	0.32670	0.00014	0.32684
150	0.87051	0.59724	0.59729	-0.00005	-0.000044	0.45557	0.00012	0.45569
165	0.96621	0.58230	0.58231	-0.00001	0.000010	0.60486	0.00011	0.60497
180	1.00000	0.57735	0.57735	0.00000	0.000000	0.74672	0.00011	0.74683

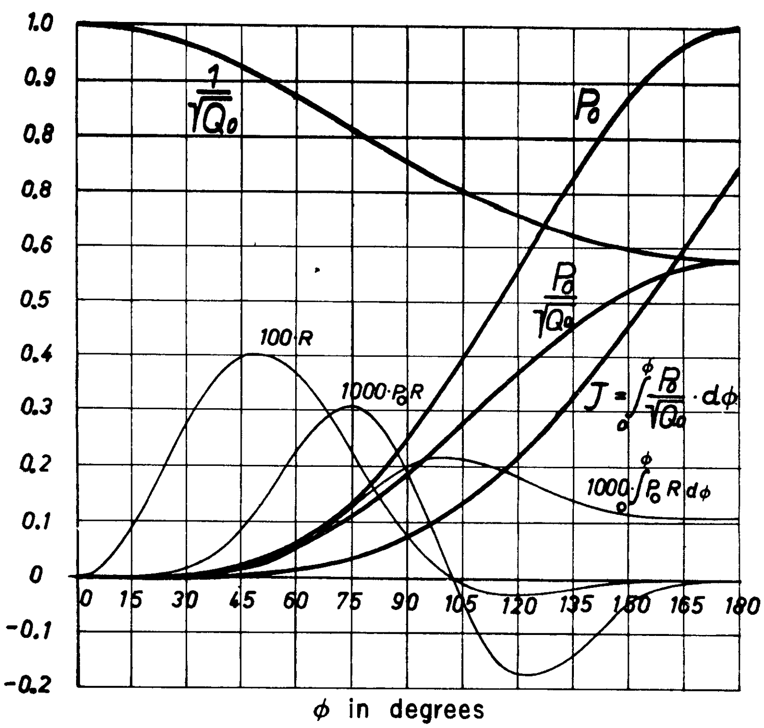

Figure 5 - Calculation of the Basic Integral $J_0 = \int_0^\phi \frac{P_0}{\sqrt{Q_0}}\, d\phi$

Now, it will be attempted to approximate $1/\sqrt{Q}$ as closely as possible by a function

$$\Omega = E + F\cos\phi + G\cos 2\phi$$

Naturally, agreement at the ends of the interval is first requisite. Then, for reasons of symmetry, the first derivatives agree also. Since P attains only small values in the beginning, the chief requirement is a good approximation towards the end of the range, and therefore agreement of the second differential quotients for $\phi = \pi$ is also essential. This gives the three definitive equations for E, F, and G.

$$E + F + G = \frac{1}{\sqrt{Q(0)}} = \sqrt{\frac{1 + \mu + \mu^2}{1 + 2\mu + 3\mu^2}}$$

$$E - F + G = \frac{1}{\sqrt{Q(\pi)}} = \sqrt{\frac{1 + \mu + \mu^2}{3 + 2\mu + \mu^2}} \qquad [33]$$

$$F - 4G = \left(\frac{1}{\sqrt{Q(\pi)}}\right)'' = \frac{3 - 2\mu - \mu^2}{4(3 + 2\mu + \mu^2)}\sqrt{\frac{1 + \mu + \mu^2}{3 + 2\mu + \mu^2}}$$

For the present example where $\mu = 0$, the right sides are 1, $1/\sqrt{3}$, and $1/4\sqrt{3}$; hence we find that

$$E = 0.771928; \quad F = 0.211325; \quad G = 0.016747$$

The approximation thus attained is very good; the maximum value of the difference

$$R = \frac{1}{\sqrt{Q}} - \Omega$$

is only about 0.004 as Figure 5 shows. Approximation is even better after multiplying by P. The maximum value of PR is 0.0003. The integral in Equation [32] is now found to be

$$J = \int_0^\phi \frac{P}{\sqrt{Q}}\,d\phi + \int_0^\phi P\Omega\,d\phi + \int_0^\phi PR\,d\phi$$

$$= \int_0^\phi (A + B\cos\phi + C\cos 2\phi)(E + F\cos\phi + G\cos 2\phi)\,d\phi + \int_0^\phi PR\,d\phi \qquad [34]$$

$$= \left(AE + \frac{1}{2}BF + \frac{1}{2}C'G\right)\phi + \left(AF + BE + \frac{1}{2}BG + \frac{1}{2}CF\right)\sin\phi$$

$$+ \frac{1}{2}\left(AG + \frac{1}{2}BF + CE\right)\sin 2\phi + \frac{1}{6}(BG + CF)\sin 3\phi + \frac{1}{8}CG\sin 4\phi + \int_0^\phi PR\,d\phi$$

The remainder of the integral can be evaluated graphically. For lower requirements of accuracy, a graphic integration of the function $P/\sqrt{Q}$ is entirely sufficient. Such treatment of the foregoing function no longer presents any difficulties, as the singular characteristics in this trigonometric configuration have vanished.

In this example, $J_0 = 0.74683$ was found for $\phi = \pi$. This was found to agree fully with the finite value determined according to a different method by Equation [21]. The functional values calculated at 15-degree intervals are shown in the table, [37].

To get the curve for the oscillation, the magnitudes calculated for the various values of ϕ,

$$t = \frac{\beta}{\mu^{5/2}} J(\phi) \text{ and } r = \frac{r_{\max} + r_0}{2} - \frac{r_{\max} - r_0}{2} \cos\phi \qquad [35]$$

must be plotted along a longitudinal or, respectively, a time axis according to Equation [32] and considering the significance of the variable $y = r/r_{\max}$ and with respect to the parameter $\mu = r_0/r_{\max}$. A series of half periods thus obtained for various values of μ are plotted in Figure 6. Even for mean values of μ, the oscillation differs strikingly from a harmonic vibration. The essential characteristic is the exceptionally sharply defined minimum in contrast to the flat maximum. Solution of the curvature of the minimum becomes almost impossible over the principal range where $0 \leqq \mu \leqq 0.1$. Furthermore, the limiting case $\mu = 0$ has a cusp at this point. Practically, the limiting case does not occur, as the latter would correspond to a point explosive charge. However, it deviates but little from the contours of the oscillations concerned. The other limiting case where $\mu = 1$ corresponds to the "sonic oscillation," owing to the fact that $r_{\max} = r_0$, and is a harmonic curve; see Section 8.

To comprehend the principal range where $0 \leqq \mu \leqq 0.1$ more conveniently, the integral J from Equation [32] can be developed again in an exponential series with respect to μ as follows:

$$\underbrace{\int_0^\phi PQ^{-1/2}\,d\phi}_{J_\mu} = \underbrace{\int_0^\phi P_0 Q_0^{-1/2}\,d\phi}_{J_0} + \mu \underbrace{\int_0^\phi (PQ^{-1/2})_0'\,d\phi}_{J_0'} + \frac{\mu^2}{2} \underbrace{\int_0^\phi (PQ^{-1/2})_0''\,d\phi}_{J_0''} + \cdots \qquad [36]$$

The desired values of P_0, Q_0, etc., can be read from Equation [32] as

$$P_0 = \frac{3}{8} - \frac{1}{2}\cos\phi + \frac{1}{8}\cos 2\phi;\; Q_0 = \frac{15}{8} - \cos\phi + \frac{1}{8}\cos 2\phi$$

$$P_0' = \frac{1}{4} - \frac{1}{4}\cos 2\phi;\; Q_0' = \frac{3}{8} + \cos\phi - \frac{3}{8}\cos 2\phi$$

$$\frac{1}{2}P_0'' = \frac{3}{8} + \frac{1}{2}\cos\phi + \frac{1}{8}\cos 2\phi;\; \frac{1}{2}Q_0'' = -\frac{3}{8} + \cos\phi + \frac{3}{8}\cos 2\phi$$

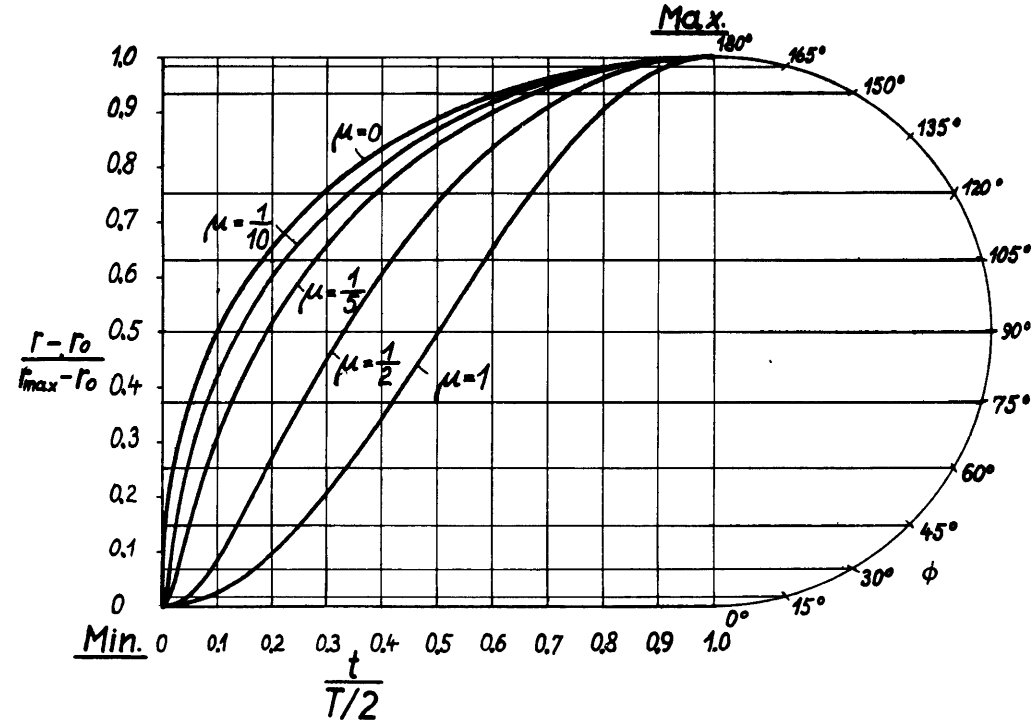

Curve of the Gas Globe Oscillation

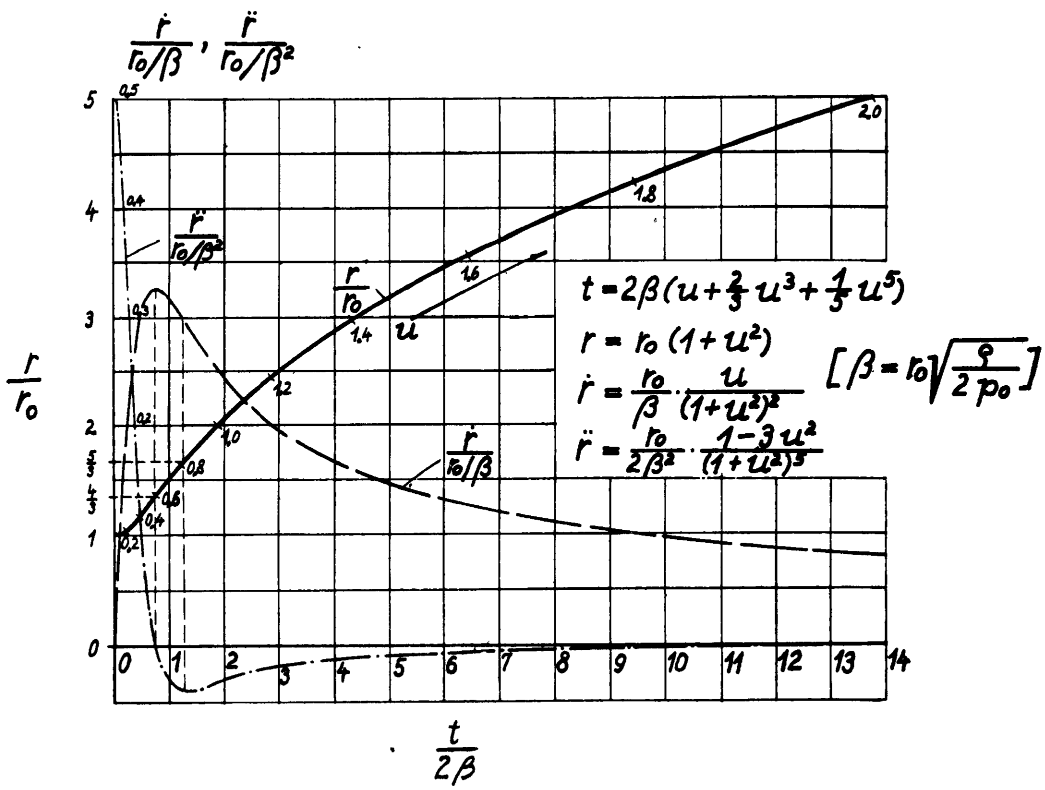

Figure 6 - Lamb's Approximation (p_a = 0)

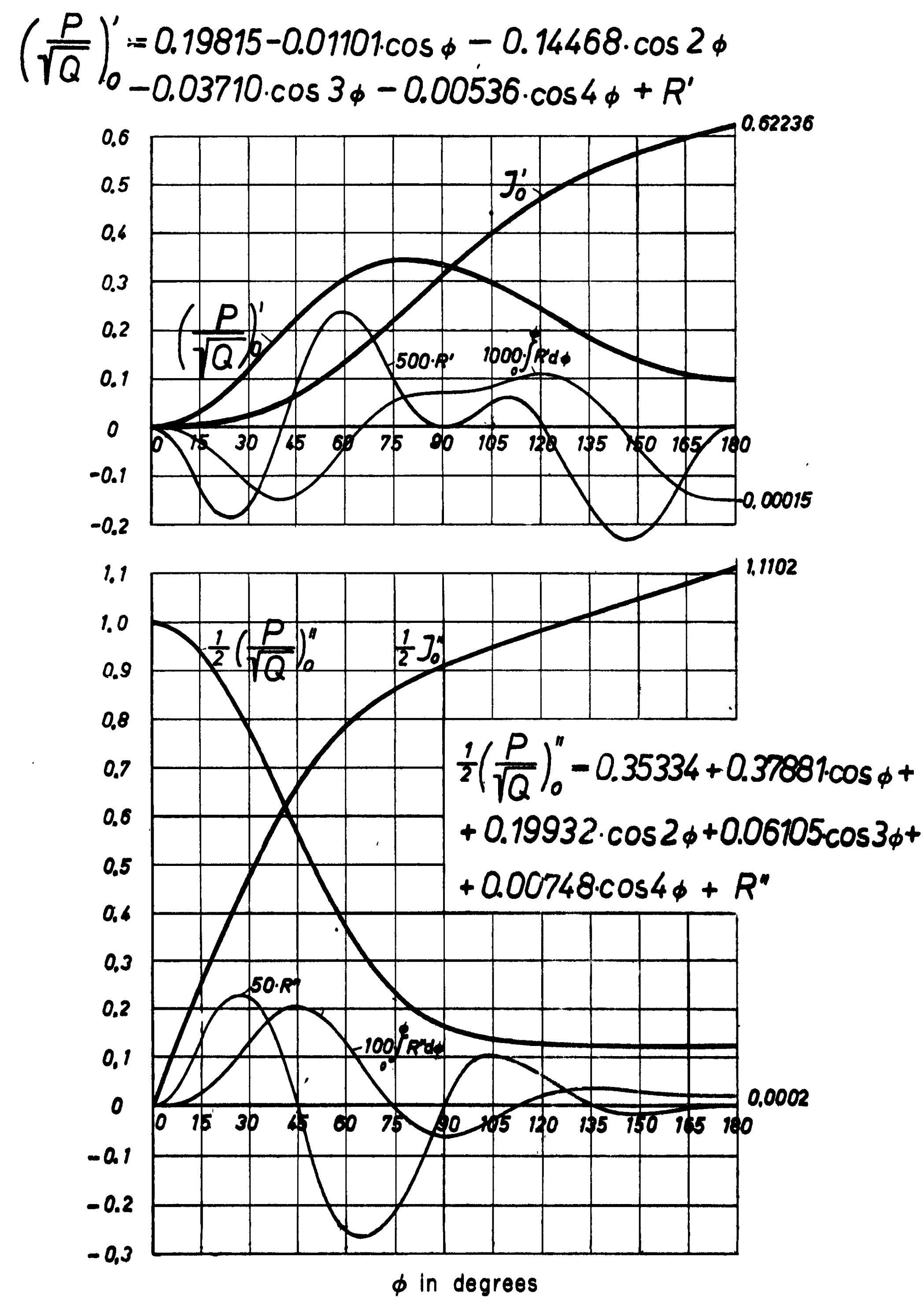

Figure 7 - Calculation of the Integrals

$$J_0' = \int_0^\phi \left(\frac{P}{\sqrt{Q}}\right)_0' d\phi \quad \text{and} \quad J_0'' \int_0^\phi \left(\frac{P}{\sqrt{Q}}\right)_0'' d\phi$$

The calculation of J_0 has been outlined already. The integrands of J_0' and J_0'' have been tabulated and approximated by cosine polynomials (to cos 4ϕ); the remainder was integrated graphically; see Figure 7. The tabulated results are

ϕ degrees	J_0	J_0'	$\frac{1}{2}J_0''$
0	0.00000	0.00000	0.0000
15	0.00002	0.00302	0.2567
30	0.00046	0.02206	0.4840
45	0.00329	0.06661	0.6615
60	0.01256	0.13634	0.7840
75	0.03390	0.22237	0.8622
90	0.07285	0.31368	0.9129
105	0.13391	0.39643	0.9506
120	0.21840	0.46716	0.9836
135	0.32684	0.52275	1.0154
150	0.45568	0.56454	1.0471
165	0.60497	0.59613	1.0787
180	0.74683	0.62236	1.1102

[37]

With the aid of this table and by Equation [36], the curve of the integral J_μ can be stated for any given (small) value of μ, and with it the curve of the oscillation can be described according to Equation [35].

7. INITIAL STAGE

The nature of the curve of motion immediately after detonation can already be recognized basically (see upper portion of Figure 6), but the solution is not sufficiently clear. A satisfactory description of the phenomenon in the initial stage can be obtained if it is considered that the work component B (see Equation [3]), which represents the effort expended in surmounting the external pressure p_a, is not significant initially and can therefore be stricken. Basically, this results in setting $p_a = 0$, as done by Lamb in the reference cited, and, according to Equation [7], this requires that α vanish. However, the time integral, Equation [9], is thereby simplified considerably, that is,

$$t = \beta \int_1^x \frac{x^{3\kappa/2}}{\sqrt{x^{3\kappa-3} - 1}}\, dx$$

and, if the radical term is set equal to μ,

$$t = \frac{2\beta}{3\kappa - 1}\int_0^u (1 + u^2)^e du \text{ with } e = \frac{8 - 3\kappa}{6(\kappa - 1)}$$

and

$$\frac{r}{r_0} = x = (1 + u^2)^{1/3(\kappa-1)} \qquad [38]$$

The integral was evaluated graphically for $\kappa = 1.2$ and 1.4; the resulting curves digress but very little from each other to $r = 3r_0$. Hence it suffices completely to consider the integrable special case where $\kappa = 4/3$. Here we find that $e = 2$ and therefore we get

$$t = 2\beta\left(u + \frac{2}{3}u^3 + \frac{1}{5}u^5\right)$$
$$r = r_0(1 + u^2) \qquad [39]$$

Agreement with the exact curve is excellent, as a later example shows; see Section 14. Graphical agreement for the first oscillation is complete to about $r = 15r_0$ and to around $r = 5r_0$ for the second oscillation, as Figure 13 shows. Equations [39] therefore suffice completely for the study of the initial motion.

The typical behavior can be seen in the lower part of Figure 6: The distance-time curve begins horizontally, according to the initial velocity $\dot{r}_0 = 0$, continues then approximately parabolic, but soon reaches the turning point

$$u = \frac{1}{\sqrt{3}}; \; t = \frac{112}{45\sqrt{3}}\beta = 1.437\beta; \; r = \frac{4}{3}r_0$$

which corresponds to the point of maximum expansion velocity. With $r \sim t^{2/5}$ it then proceeds to infinity. Hence the periodicity of the oscillation is lost, owing to the lack of external pressure.

The curve can be regarded somewhat as the infinitely magnified embryo of the type of oscillation pertaining to $\mu = 0$ and shown in the upper portion of Figure 6.

8. SONIC OSCILLATION OF GAS GLOBES

The other limiting case is represented by $\mu = 1$ and, since $r_0 = r_{max}$, can be designated as the sonic oscillation of gas globes. The integral expression, Equation [32], valid for the special case where $\kappa = 4/3$, then becomes elementary as

$$t = \beta \int_0^{\phi} \frac{d\phi}{\sqrt{2}} = \frac{\beta}{\sqrt{2}} \phi$$

because $P = 1$ and $Q = 2$. The oscillation proceeds simply as a harmonic with respect to Equation [35] and its period is

$$T_1 = \beta\sqrt{2}\,\pi = r_0 \pi \sqrt{\frac{\phi}{p_0}} \qquad [40]$$

The case for κ, in general, can also be solved, if, after performing the trigonometric substitution, we traverse to the limit $\mu \to 1$ in Equation [31]. The calculation is somewhat difficult, as three differentiations (l'Hospital's law) have to be made to eliminate the indeterminate character of Q.

Finally, the limiting value,

$$\lim_{\mu \to 1} Q = \frac{9}{2}\kappa(\kappa - 1)$$

is found, which is not a function of ϕ. Thereby t becomes linear in ϕ, and the oscillation is again harmonic as Minnaert assumes from the outset; see the reference cited. In agreement with him,

$$T_1 = r_0 \pi \sqrt{\frac{4\phi}{3\kappa p_0}} \qquad [41]$$

is found for the oscillation period. This value is of importance for present purposes insofar as it represents a natural reference magnitude for the following comparison of oscillation periods.

9. COMPARISON OF VARIOUS CONDITIONS OF OSCILLATION OF THE SAME GAS GLOBE

A gas globe of radius r_a with an internal pressure $p = p_a$ in a state of stable or stationary equilibrium is assumed. With $\kappa = 4/3$, let the gas globe be compressed adiabatically to the condition r_0, p_0 and then released. The intensity of the compression can be characterized by μ or by the "expansion factor" $m = 1/\mu = r_{max} : r_0$; see Equation [12]. According to the adiabatic relationship, Equation [2],

$$p_0 = p_a \left(\frac{r_a}{r_0}\right)^{3\kappa} = p_a \left(\frac{r_a}{r_0}\right)^4 \qquad [42]$$

Now, however, according to Equations [7] and [13],

$$\frac{p_0}{p_a} = \frac{1}{3\alpha^3} = \frac{1}{3}(m + m^2 + m^3) \approx \frac{1}{3}m^3 \quad \text{(for large } m\text{)} \qquad [43]$$

Therefore,

$$\frac{r_a}{r_0} = \sqrt[4]{\frac{1}{3}(m + m^2 + m^3)} \approx \frac{1}{\sqrt[4]{3}} m^{3/4} \qquad [44]$$

and

$$\frac{r_{\max}}{r_a} = \frac{m}{\sqrt[4]{\frac{1}{3}(m + m^2 + m^3)}} \approx \sqrt[4]{3}\, m^{1/4} \qquad [45]$$

The oscillation period determined by Equation [19]

$$T = \frac{2\beta}{\mu^{5/2}} J_\mu = r_0 \sqrt{\frac{2\rho}{p_0}} J_\mu m^{5/2}$$

will now be compared with the sonic oscillation period found by Equation [40] as

$$T_1 = r_0 \pi \sqrt{\frac{\rho}{p_a}}$$

The result is found to be

$$\frac{T}{T_1} = \frac{\sqrt{2}}{\pi}\left(\frac{r_0}{r_a}\right)^3 J_\mu m^{5/2} = \frac{J_\mu \sqrt[4]{108}}{\pi} \sqrt{\frac{m^7}{(1 + m + m^2)^3}} \approx \frac{J_\mu \sqrt[4]{108}}{\pi} m^{1/4} \qquad [46]$$

By Equations [43] and [46], all magnitudes concerned which are of interest are now expressed as parameters by the expansion factor m. They are plotted in Figure 8 for $m = 1$ to 100 on double logarithmic coordinates. The asymptotes of the curves are represented by the equations of approximation included. The equations have also been plotted in simple logarithmic coordinates for greater clarity; see Figure 9. Here the required values of J_μ are found also, which were determined by the trigonometric method, for larger values of m with the aid of Equation [29]; see Section 6.

The range of the first oscillation of the gas globe coming into consideration is around $m = 30$, as already mentioned. For the second oscillation, the values can be considered to lie below 10.

It would be desirable to extend this useful presentation to other values of κ also; compare Section 14.

10. VELOCITY AND ACCELERATION CURVES

The velocity $\dot{r}$ of the gas globe front, when the nondimensional coordinate $x = r/r_0$ according to Equation [8] is used, is described by the expression

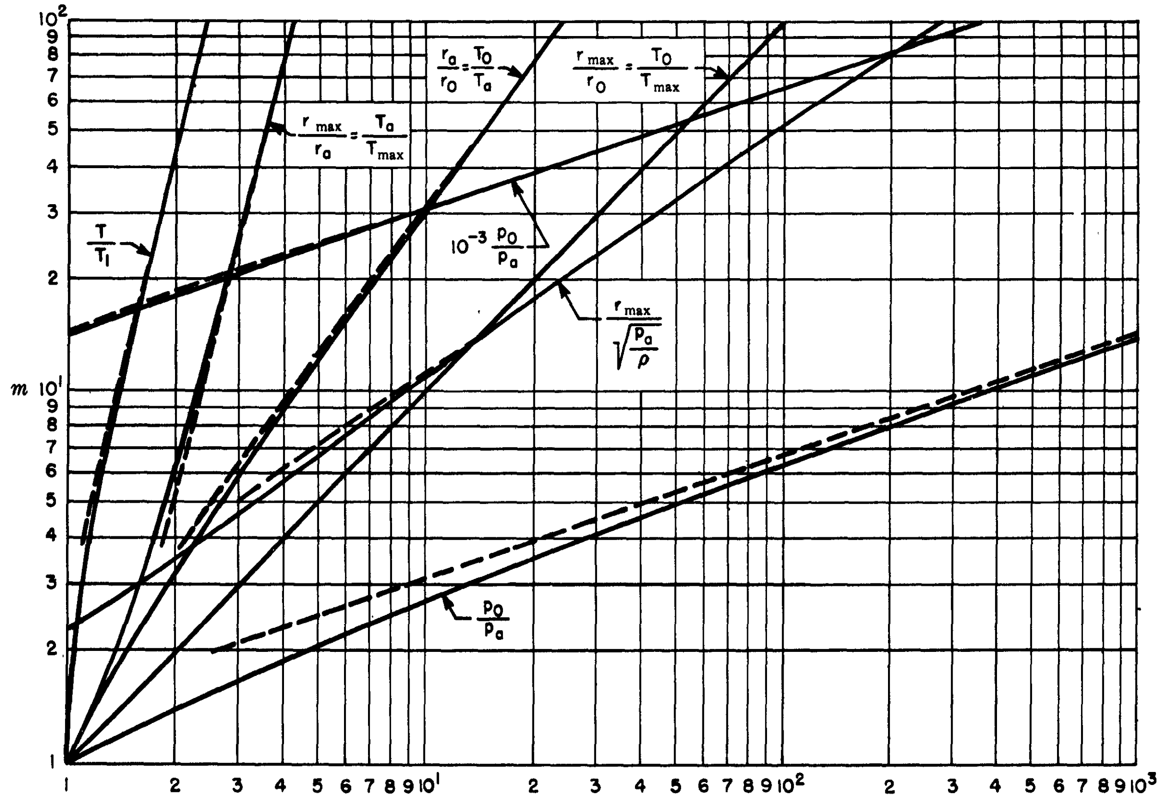

Figure 8 - Comparison of Various Conditions of Oscillation for the Same Gas Globe (where $\kappa = 4/3$)

$$\beta^2 x^2 = (1 + \alpha^3)x^{-3} - x^{-3\kappa} - \alpha^3$$

with

$$\alpha^3 = (\kappa - 1)\frac{p_a}{p_0} \qquad \text{and} \qquad \beta^2 = 3(\kappa - 1)\frac{\rho r_0^2}{2p_0}$$

By differentiating twice with respect to t, the following expressions

$$2\beta^2 \ddot{x} = 3\left\{-(1 + \alpha^3)x^{-4} + \kappa x^{-3\kappa-1}\right\}$$

$$2\beta^2 \dddot{x} = 3\dot{x}\left\{4(1 + \alpha^3)x^{-5} - \kappa(3\kappa + 1)x^{-3\kappa-2}\right\}$$

are found successively. After multiplying by r_0, the following equations for kinematic magnitudes are thus found to be

$$\text{Velocity} \quad \dot{r} = \frac{r_0}{\beta}\sqrt{(1 + \alpha^3)x^{-3} - x^{-3\kappa} - \alpha^3}$$

$$\text{Acceleration} \quad \ddot{r} = \frac{3r_0}{2\beta^2}\left\{-(1 + \alpha^3)x^{-4} + \kappa x^{-3\kappa-1}\right\} \qquad [47]$$

$$\text{Jerk} \quad \dddot{r} = \frac{3\dot{r}}{2\beta^2}\left\{4(1 + \alpha^3)x^{-5} - \kappa(3\kappa + 1)x^{-3\kappa-2}\right\}$$

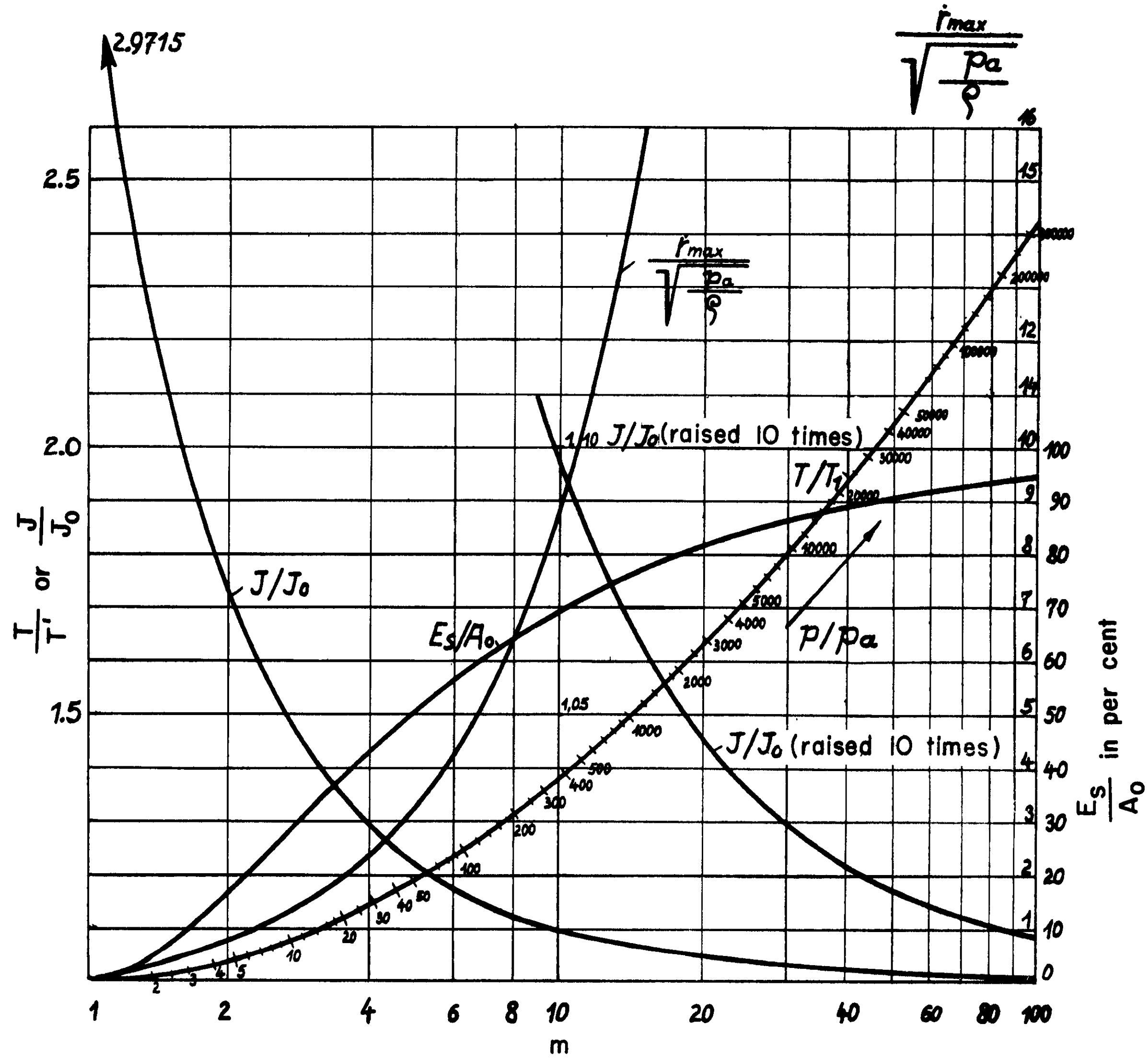

Figure 9 - Comparison of Various Conditions of Oscillation for the Same Gas Globe (where κ = 4/3)

According to assumptions, the initial velocity r_0 is equal to zero, as is found by substituting x = 1 into Equation [47]. Now, the velocity rises rapidly, as the initial acceleration is very high; see Figure 6, that is,

$$\ddot{r}_0 = \frac{3r_0}{2\beta^2}(\kappa - 1 - \alpha^3) = \frac{p_0 - p_a}{\rho r_0} \qquad [48]$$

The initial acceleration is inversely proportional to the cube root of the weight of the explosive charge and in the order of magnitude of approximately 2×10^7 m/sec^2 or about 2×10^6 g for 1 kg of explosive charge, where g denotes the acceleration of gravity.

As the globe expands, the acceleration decreases at first. The instant at which it vanishes corresponds to the point of inflection on the distance-time curve and is related to maximum velocity:

$$r = r_0\left(\frac{\kappa}{1+\alpha^3}\right)^{1/(3\kappa-3)} \approx r_0\kappa^{1/(3\kappa-3)}\left(=\frac{4}{3}r_0 \text{ for } \kappa = \frac{4}{3}\right) \qquad [49]$$

$$\dot{r}_{\max} = \frac{r_0}{\beta}\sqrt{(\kappa-1)\left(\frac{1+\alpha^3}{\kappa}\right)^{\kappa/(\kappa-1)} - \alpha^3} \approx \sqrt{\frac{2p_0}{3\rho\kappa^{\kappa/(\kappa-1)}}}\left(=\frac{3}{8}\sqrt{\frac{3p_0}{2\rho}}\right)$$

The maximum velocity of expansion is not a function of the size of the charge and is nearly independent of the charge depth. It is about 450 m/sec.

The acceleration decreases further and becomes negative; the velocity decreases accordingly. The maximum retardation is attained at vanishing jerk, that is

$$r = r_0\frac{\kappa(3\kappa+1)^{1/(3\kappa-3)}}{4(1+\alpha^3)} \approx r_0\left[\frac{\kappa}{4}(3\kappa+1)\right]^{1/(3\kappa-3)}\left(=\frac{5}{3}r_0 \text{ for } \kappa = \frac{4}{3}\right) \qquad [50]$$

$$-\ddot{r}_{\max} = \frac{9r_0}{8\beta^2}\kappa(\kappa-1)\left[\frac{4(1+\alpha^3)}{\kappa(3\kappa+1)}\right]^{\frac{3\kappa+1}{3\kappa-3}} \approx \frac{3\kappa p_0}{4\rho r_0}\left[\frac{4}{\kappa(3\kappa+1)}\right]^{\frac{3\kappa+1}{3\kappa-3}}\left(=\left(\frac{3}{5}\right)^5\frac{p_0}{\rho r_0} \approx \frac{1}{13}\ddot{r}_0\right)$$

Quantitatively, this retardation or deceleration is approximately 1/13 the initial acceleration.

From here on, the retardation again decreases and reaches its extreme at the stage of the globe maximum at vanishing velocity. In analogy to Equation [48] and with consideration for Equation [2],

$$\ddot{r}_m = \frac{p_{\min} - p_a}{\rho r_{\max}} \text{ with } p_{\min} = p_0\mu^{3\kappa} \qquad [51]$$

Quantitatively, by order of magnitude, this deceleration is 1/200,000 of $\ddot{r}_0$; i.e., for a charge of 1 kg it is 10 g.

The approximations indicated in Equations [49] and [50] for small values of p_a are found by neglecting α. They agree, therefore, with those values which would be obtained within the scope of Lamb's approximation which sufficed to satisfy conditions for the initial stage; see Section 7.

If $\dot{r}_{\max}$ is referred to the velocity term $\sqrt{p_a/\rho}$ which is a function of the external pressure, a value, which is a function of α or m only, can be found for a given value of κ with the aid of Equation [49]. For $\kappa = 4/3$, this value is

$$\frac{\dot{r}_{\max}}{\sqrt{p_a/\rho}} = \sqrt{\frac{9}{128}\alpha^{-3}(1+\alpha^3)^4 - \frac{2}{3}} \approx \frac{3}{8\sqrt{2}}m^{3/2} \qquad [52]$$

and is plotted in Figures 8 and 9 as a function of m. The approximate value again gives the asymptote. After computation of $\sqrt{p_a/\rho}$, these curves permit easy reading of the maximum velocity of any given globe oscillation. As can be seen, the velocity for the sonic oscillation is zero and rises with increasing amplitude to values of any desired magnitude.

11. TRANSFER OF ENERGY

As shown in the introduction, the capacity for work A of the gas globe has its maximum value A_0 in its initial stage, the so-called gas globe energy. During expansion of the globe, the capacity for work decreases continuously, as it is converted into the work of displacement B and kinetic energy E. The study of the curve as a function of the radius of the globe r is already possible with the aid of Equations [1], [2], and [3] and the energy expression

$$A_0 = A + B + E$$

If, for purposes of comparison, all factors are related to A_0 and the nondimensional coordinate $x = r/r_0$ is used, then

$$\frac{A}{A_0} = \frac{pV}{p_0V_0} = \left(\frac{V_0}{V}\right)^{\kappa-1} = \frac{1}{x^{3\kappa-3}}$$

$$\frac{B}{A_0} = \frac{(\kappa - 1)p_a}{p_0}\left(\frac{V}{V_0} - 1\right) = \alpha^3(x^3 - 1) \qquad [53]$$

$$\frac{E}{A_0} = 1 - \frac{A}{A_0} - \frac{B}{B_0} = 1 - x^{3-3\kappa} - \alpha^3(x^3 - 1)$$

The curve for the first and second oscillations of a 5-gm explosive charge is shown in Figure 14; see Section 14. The typical behavior can be recognized: A decreases constantly according to a sort of equilateral hyperbola; B increases according to a sort of cubical parabola, not noticeably at first, then with greater and greater speed; and E rises rapidly from zero to a maximum, whereupon it drops in turn more slowly back to zero. At this instant, at the maximum of the gas globe, the motion reverses and the energy curves now run in the opposite direction, theoretically back to the initial value, but practically, however, this is not quite true.

The energy change with respect to time, due to the now familiar expansion curve of the gas globe having such sharply defined minima, is especially abrupt in the vicinity of the latter. The change of A and E occurs with such lightning speed that it is scarcely possible to plot it by usual methods; see Figure 13. The time scale must be extended considerably; see

Figure 14. Then, using this smaller time base, Lamb's development given in Section 7 can be used.

The instant of the maximum kinetic energy, ordinarily designated as "thrust energy" $E_{max} = E_S$, is of interest. The latter is decisive for the so-called close-range effect, that is, the destructive effect of an underwater detonation in close proximity to the point of detonation. This moment is characterized by the pressure balance $p = p_a$, as already explained at the end of Section 2. The corresponding "balance radius" r_a is found simply from the adiabatic equation, Equation [2] or [42], as

$$r_a = r_0 \sqrt[3\kappa]{\frac{p_0}{p_a}} \qquad [54]$$

Therefore, for the thrust energy and considering Equation [7] it follows from the foregoing that

$$\begin{aligned} \frac{E_S}{A_0} &= 1 - \kappa\left(\frac{p_a}{p_0}\right)^{(\kappa-1)/\kappa} + (\kappa - 1)\frac{p_a}{p_0} \\ &= 1 - \frac{\kappa}{(\kappa - 1)^{(\kappa-1)/\kappa}}\,\alpha^{(3\kappa-3)/\kappa} + \alpha^3\left(= 1 - \underbrace{\frac{4}{3}\sqrt[4]{3}}_{1.753}\,\alpha^{3/4} + \alpha^3 \text{ for } \kappa = \frac{4}{3}\right) \end{aligned} \qquad [55]$$

For small values of α, the quantity E_S obviously will not be very much smaller than A_0. The exact curve for κ = 1.2 to 1.4 as a function of μ is plotted in Figure 10. The curve for $\kappa = 4/3$ is also plotted as a function of m in Figure 10. It can be seen that, as the expansion factor increases, a rising proportion of the capacity for work of the explosive charge A_0 is converted into kinetic energy. For the first oscillation resulting from the detonation of a 5-gm charge of TNT (Section 14), which will be treated later, this portion amounted to approximately 86 per cent, for example, assuming $\kappa = 4/3$.

12. CHANGE OF TEMPERATURE

The absolute temperature τ of a gas with known gas constant R, and a given pressure p and volume V is determined by the general equation of state

$$\frac{pV}{\tau} = LR = \text{constant} \qquad [56]$$

For the products of combustion of the explosive, R is given indirectly by the "specific gas volume" v_G which characterizes the space required by the products of combustion produced by the detonation of 1 kg of explosive charge at a normal pressure of 760 mm of mercury ($p \approx 1$ atm) and 0 degree C (τ = 273 degrees abs)

$$R = \frac{v_G}{273}$$

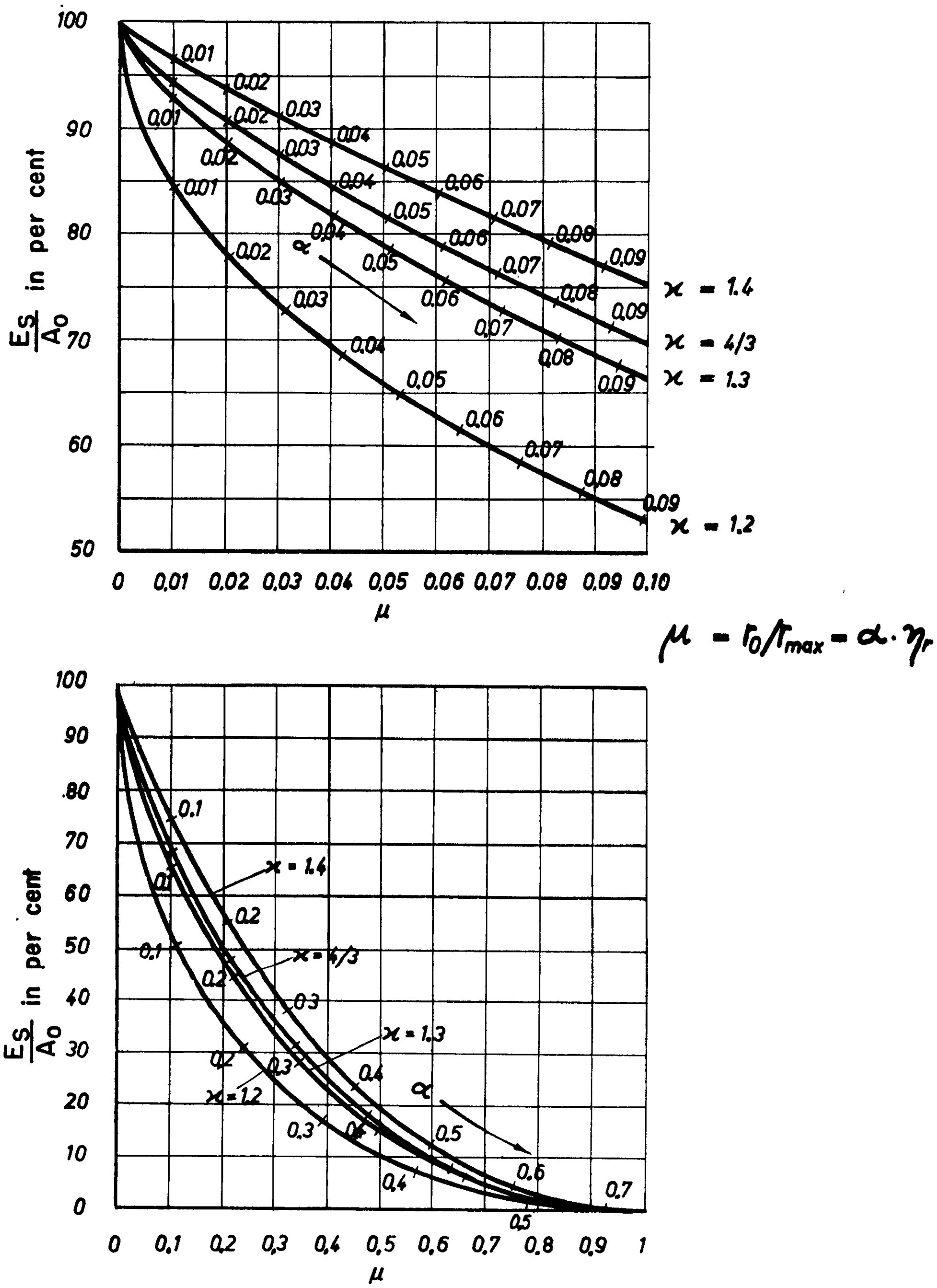

Figure 10 - Component of Thrust Energy E_S in the Capacity for Work A_0

With the foregoing, the initial temperature is found to be

$$\tau_0 = \frac{p_0 V_0}{LR} = \frac{273 p_0}{s v_G} \qquad [57]$$

For the adiabatic change of state of the gas globe in Equation [2], the temperature law

$$\tau V^{\kappa - 1} = \text{constant}$$

follows from Equation [56]. If Equation [56] is compared with Equation [1], the ratio of the absolute temperature τ to the capacity for work A, described by the first expression under Equation [54], can be recognized as

$$\frac{\tau}{\tau_0} = \frac{A}{A_0} = \left(\frac{r_0}{r}\right)^{3\kappa-3} \qquad [58]$$

For $\kappa = 4/3$, it follows that the special absolute temperature and the capacity for work are inversely proportional to the radius of the globe. The temperature range for the curve of one oscillation is accordingly very great. The temperature changes initially and in the zone of the minima at lightning speed equivalent to A; see Sections 10 and 11. The temperature curve for the example of the 5-gm explosive charge given in conclusion is shown in Figure 16.

13. COMPARISON WITH MEASUREMENTS

The validity of the laws required by theory for the maximum gas globe radius, Equation [18], and the period of oscillation, Equation [30], will be checked by measured data.

First, explosion tests were made with small charges of TNT, S1,* and PETN. They were made at a depth of 1 m in a tank and were photographed with a high-speed camera at a rate of 1000 to 1500 frames per second. The charges weighed 5, 10, 15, and 20 gm, to which the weight of the incandescent igniter, 1/2 gm (0.9 gm tetryl + 0.3 gm lead azide), must be added. The films show the repeated oscillation of the gas globe very nicely. Naturally, however, in contrast to the theory developed herein, the oscillation is damped. The curve for a single oscillation is reproduced very well by the theory until it reaches the vicinity of the minima where evaluation of the films is hardly possible, as the water is obscured and soiled due to the sooty sludge produced by the solid residual products of combustion resulting from detonation. Therefore, the outline of the gas globe cannot be distinguished; compare Section 14. The gas globe itself is almost perfectly spherical during the first oscillation, as evident in Figure 1, but is deformed somewhat by buoyancy toward the end of the second oscillation.

To check Equations [18] and [30], namely,

$$r_{\max} = c_r \sqrt[3]{\frac{L}{p_a}}, \quad T = C_T \sqrt[3]{\frac{L}{{p_a}^{2.5}}}$$

---

* Translator's Note: S1 is an explosive developed by the CPVA. It consists of 60 per cent TNT, 24 per cent HND, and 16 per cent powdered aluminum.

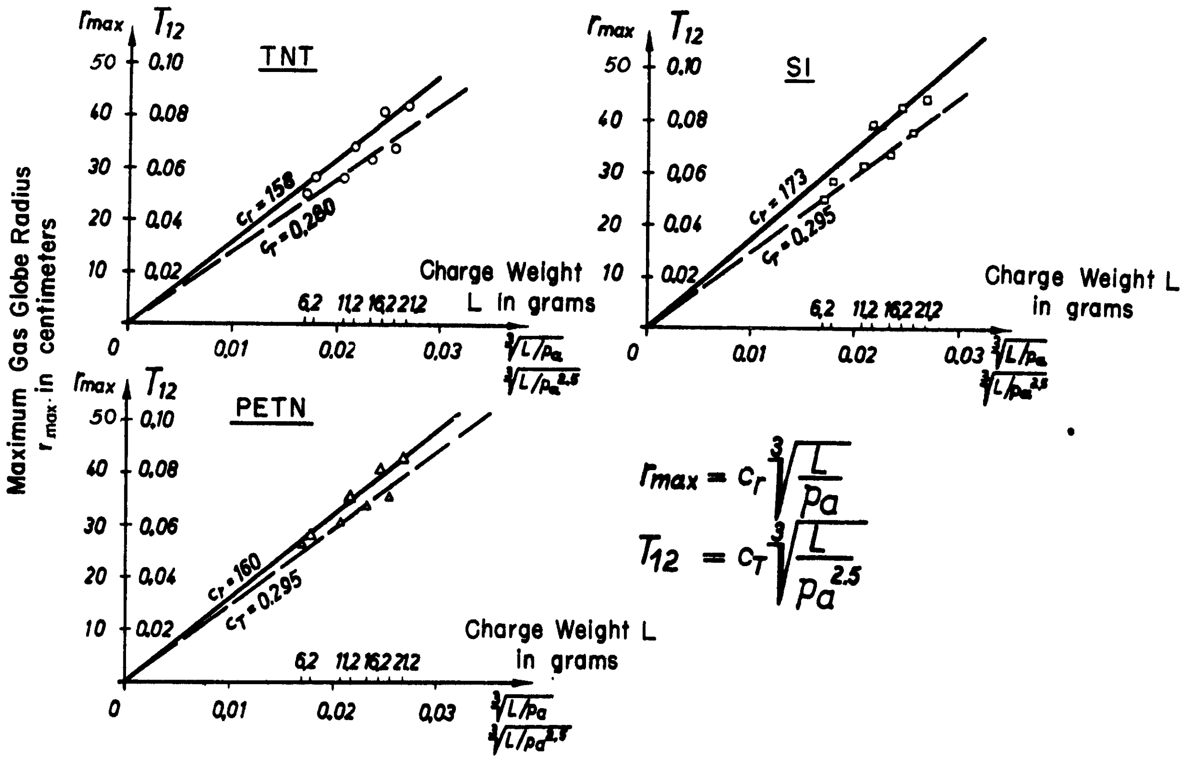

Figure 11a - Detonations of 5-, 10-, 15-, and 20-Gram Charges with 1.2-Gram Igniters Each Set in Water 1 Meter Deep

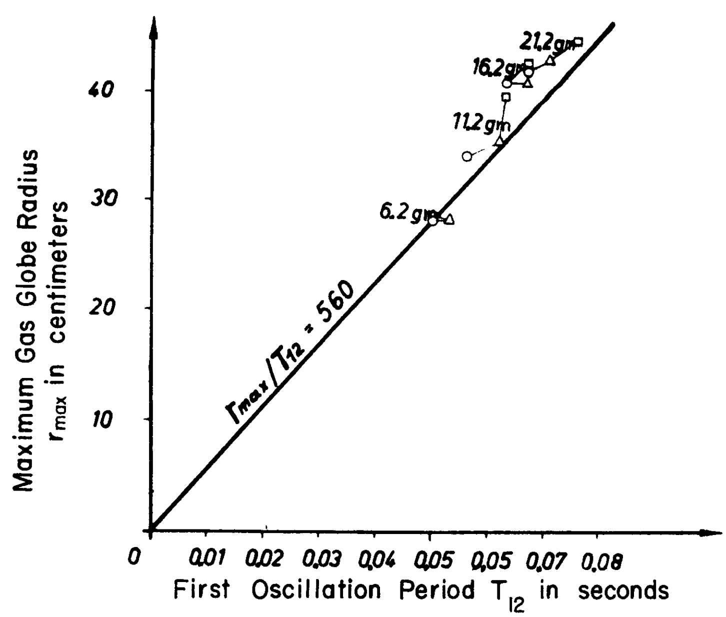

Figure 11b - Ratio of Maximum Gas Globe Radius to the First Oscillation Period

Figure 11 - Comparison of Measurements with Theory

which can be held valid for the first oscillation only, the maximum radii r_{max} and the first oscillation periods T_{12} were taken from earlier tests and plotted as functions of the corresponding cube roots (with L = 6.2, 11.2, 16.2, and 21.2 gm, respectively, and p_a = 1.1 atm); see Figure 11. For each type of explosive, the respective points would have to lie on a linear curve traversing the origin, whose slope corresponds to the value of the constants c_r or c_T.

It is evident from the foregoing that the points scatter somewhat. This can be attributed primarily to the proximity to the surface and the nonhomogeneity of the charges. Mean curves give the following tabulated values:

	TNT	S1	PETN
c_r	158	173	160
c_T	0.280	0.295	0.295

If T_{12} and r_{max} are plotted in two perpendicular directions, that is, in rectangular coordinates, the plotted points would have to lie on a linear curve also whose slope is given by Equations [18] and [30] as

$$\frac{r_{max}}{T} \approx \sqrt[3]{\frac{3}{4\pi}} \frac{\sqrt{p_a}}{0.00114577} = 541.44\sqrt{p_a} \qquad [59]$$

With p_a = 1.1 atm, and after deduction of a correction of 1 per cent as required by η_r, this gives a value of about 560. As can be seen from Figure 11, these small charges satisfy this condition more or less well, whereas measured values for larger charges are without exception above the linear curve corresponding to the value of 560. In any case better agreement with theory can be expected for smaller charges because, owing to smaller gas globes and slower motion of the water, effects of free surface and wall effects are not as highly apparent in tank tests.

As the experimental relation between the gas globe and the period of the first oscillation has been found to be in agreement with theoretical values to this point, an independent test of both principal relationships, Equations [18] and [30], resulting from this theory can now be made. The measurement of the gas globe radius is difficult for larger charges, and as the special method based on soundings is required, such measurement ceases to be accurate; see Reference (7).

Despite the foregoing, Ramsauer's values for wet guncotton (7) will be given in Table 1. The calculated values were found by Equation [18] and with a mean value of c_r = 1.593. This table shows "how unexpectedly accurate is the agreement of this formula with tests 1 to 10."

TABLE 1

Maximum Gas Globe Radius (Observed and Calculated)

Number	L kg	p_a atm	C_r	Observed Radius r_{obs} cm	Calculated Radius r_{cal} cm	$r_{cal} - r_{obs}$
1	1.910	1.2	1.585	185	186.0	+ 1.0
2	1.910	1.3	1.593	181	181.1	+ 0.1
3	1.910	1.6	1.603	170	169.0	- 1.0
4	1.910	1.9	1.548	155	159.6	+ 4.6
5	0.910	1.3	1.587	141	141.4	+ 0.4
6	0.455	1.3	1.602	113	112.3	- 0.7
7	1.910	1.3	1.602	182	181.1	- 0.9
8	1.070	1.3	1.578	148	149.3	+ 1.3
9	1.070	1.3	1.621	152	149.3	- 2.7
10	1.910	1.3	1.610	183	181.1	- 1.9

The period of the oscillation of the gas globe can be measured far more accurately than the radius of the gas globe. An underwater microphone is used in this case, which responds to the pressure waves radiated from the gas globe minima; the surges of electrical current induced are recorded with an oscillograph; see Figure 17. By using sufficiently high film speeds, a satisfactory deceleration of the phenomenon is attained, permitting maximum measuring accuracy. It should be emphasized that under exactly identical conditions, that is, by detonation of explosive charges of identical weight and composition, periods of oscillation were found by precision measurements which diverged from one another by approximately 0.3 per cent only. This accuracy cannot usually be attained in explosion tests. Therefore, an especially accurate proof of the theory developed must be possible, by checking or verifying the formula for the "impact time."

With a series of identical charges detonated in a lake 100 to 120 m deep, the period of oscillation of the gas globe as a function of the charge depth was measured. Charges were used consisting of 100 $\pm$ 0.1 gm of a cast mixture composed of 45 per cent TNT and 55 per cent RDX. This mixture guaranteed complete detonation, even without a special booster charge. The oscillation periods measured appear in Table 2.

The mean oscillation periods derived from groups of four measurements each were plotted on double logarithmic paper as shown in Figure 12.

TABLE 2

Impact Time as a Function of the Charge Depth, Measured with 100-Gram Charges, Composed of 45 Per Cent TNT Admixed with 55 Per Cent RDX

Explosive Depth m	Air Pressure during Measurement mbar	p_a mbar	T_1 millisec				T_1 Mean Value millisec
1	931	1029	120.1	121.0	120.9	121.8	121.0
1.5	930	1077	124.0	123.7	124.8	122.9	123.9
2	935	1131	122.9	122.3	122.2	122.6	122.5
2.5	934	1179	120.2	120.3	120.3	120.6	120.3
3	925	1219	118.7	118.4	118.2	116.6	118.0
4	926	1318	112.6	112.2	112.2	112.2	112.3
5	930	1420	106.0	105.9	107.2	106.0	106.2
7	920	1606	96.1	97.9	95.2	96.1	96.3
10	925	1906	83.6	83.5	83.6	83.7	83.6
15	928	2399	69.3	68.8	68.9	69.2	69.1
20	939	2900	59.3	58.3	59.3	59.4	59.1
30	937	3879	46.0	46.0	46.0		46.0
40	937	4860	37.9	38.2	38.1	38.1	38.1
55	921	6315	30.4	30.5	30.5	30.4	30.4
70	931	7796	25.7	25.6	25.1		25.5

The measured values obtained for greater charge depths lie exactly on the plotted linear curve whose slope is -5/6, corresponding to the theoretical value. Equation [30] may therefore be regarded as absolutely confirmed. A deviation from the linear curve does not occur until the surface is approached. In the present case, the disturbance can barely be perceived at around 10-m charge depth; the maximum radius of the gas globe is therefore in this case approximately 0.75 m.

The second proof of Equation [30] still possible for the period of oscillation of the gas globe consists in varying the quantity of explosive charge at constant depth. Precautions must be taken to avoid the zone of surface disturbance when detonating the charges. For the measurements shown in Figure 12, using 0.1- to 10-kg charges at 50-m charge depth and approximately 100-m depth of water, undisturbed conditions prevailed. Excluding measured data for charges of larger scale, where the casings constituted a disturbing factor, the plotted results lie on a linear curve having a slope of 1/3. Therefore, the ratio of the impact time to the cube root of the

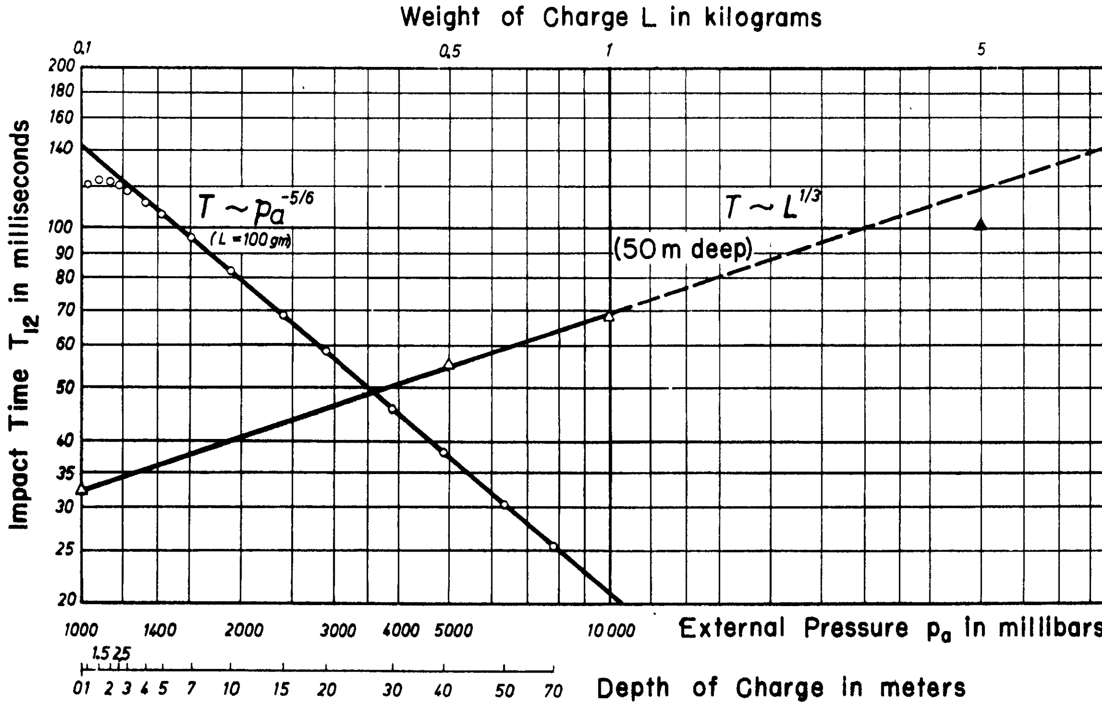

Figure 12 - Impact Time as a Function of the Size of the Charge and of the Charge Depth

These precision measurements were made with a mixture consisting of 45 per cent TNT admixed with 55 per cent RDX.

quantity of explosive charge is valid for undisturbed cases. In summarizing, it can therefore be stated that the equation for impact time, resulting from the theory just developed, is satisfied completely for undisturbed cases.

14. APPLICATION TO AN EXAMPLE

Now that the formulas derived from theory for the maximum radius of the gas globe and the period of the oscillation have been checked in detail on the basis of the test data at hand and have proved very reliable, these theories will be applied to an individual example. The application of the mathematics and curves given will be demonstrated at the same time. For this purpose, the detonation of 5 gm of TNT plus a 1.2-gm incandescent igniter will be used, which promises good agreement on the basis of earlier tests of the ratio $r_{max} : T$ according to Equation [59] and Figure 11.

The given values to be considered are:

Weight of the Charge	$L = 6.2$ gm $= 0.0062$ kg
Density of the Explosive	$s' = 1.58$ gm/cm^3, $\quad s = 0.00158$ kg/cm^3
External Pressure	$p_a = 1.1$ atm

Furthermore, the value $\kappa = 4/3$ will be used.

a. FIRST OSCILLATION

From the measured maximum radii for four charges of TNT, the familiar value of the "constant" $c_r = C_r/\eta_r$ in Equation [18] is found to be 158 according to Figure 11. Thereby we find the initial pressure

$$p_0 = 8700\ \eta_r^3$$

If the correction factor η_r is next set equal to 1 from Equation [7], we find $\alpha \approx 0.0348$ in the first approximation to which $\eta_r = 1.012$ pertains according to Figure 3. This permits the improved values

$$p_0 = 9020 \text{ atm}; \quad \alpha = 0.0344; \quad \beta = 7.35 \cdot 10^{-6}$$

Repetition of this process gives no further changes. Thus the actual constant of the explosive is found to be $C_r = 160$. From Equations [12] and [14] the

Expansion Factor $m = 28.7$ and its Reciprocal $\mu = 0.0348$

result, which could also be found directly by Equations [17] and [18] from the

Maximum Radius of the Globe $r_{max} = 28.1$ cm

and from the

Radius of the Explosive $r_0 = 0.978$ cm

Equation [22] gives the impact-time constant $C_T = 0.295$ and Figure 4 gives the correction factor $\eta_r = 1.0008$, which has to be neglected. When $\gamma = 1$, it follows that the

Period of Oscillation $T = 0.0501$ second

which is in complete agreement with the experiment.

The curve plotted in Figure 13 for the first oscillation was found according to Equation [35] for which the integral J_μ was developed with the aid of the tabulation (Equation [37]) and by Equation [36] for $\mu = 0.0348$. The agreement of the measured points with the theoretical curve is very good with the exception of the vicinity of the minimum, a fact mentioned on several occasions. These points are inaccurate because the sooty products of combustion prevent the globe outline from being distinguished. The initial stage of the expansion of the globe was described according to Lamb, Equation [39], and shows graphic agreement to about $r = 15r_0$; see Figures 13 and 14.

Figures 14 and 15 show the relative velocity curve according to Equation [47], first as a function of the radius of the globe, second as a function of time. From Equations [48], [49], [50], and [51], the following values are found:

Maximum Velocity $\dot{r}_{max} = 432$ m/sec
Initial Acceleration $\ddot{r}_0 = 90.4 \times 10^6$ m/sec^2 $= 9.22 \times 10^6$ g

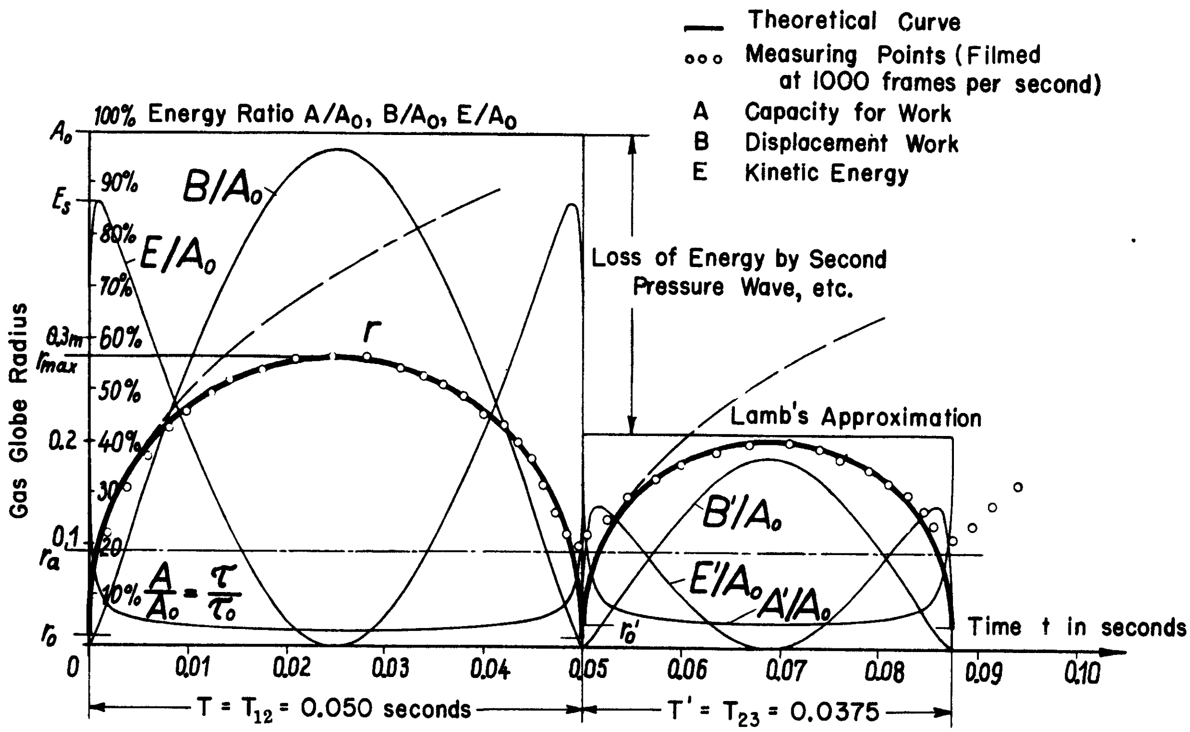

Figure 13 - Oscillation of the Gas Globe Produced by Detonating 5 + 1.2 Grams of TNT at a Charge Depth of 1 Meter

Maximum Deceleration $\ddot{r}_{max}$ = -7.03 × 10^6 m/sec^2 = -0.717 × 10^6 g
Final Deceleration $\ddot{r}_m$ = -379 m/sec^2 = -38.6 g

In Figures 13, 14, and 15, the transfer of energy is shown according to Equation [47]. The reference magnitude is, according to Equations [1] or [60], the initial

Capacity for Work A_0 = 1062 kg-m = 2.487 kg-cal

As shown in Figure 15, approximately 86 per cent is converted into thrust energy E_S. Based on the specific energy of detonation, which amounts to 840 kg-cal/kg for TNT, a total energy of 5.21 kg-cal can be ascribed to the explosive charge herein concerned. If this value is compared with A_0, it might be assumed that 52.2 per cent of this energy was radiated with the first pressure wave. However, this is not quite true, as on the basis of the pressure curve of the explosive pressure wave measured in water for TNT, the pressure wave contains a somewhat smaller percentage of explosive energy. Accurate numerical values cannot be given yet. Considering this, it must be emphasized that the initial pressure p_0 = 9020 atm, calculated in the beginning, represents only a fictitious value and will be much higher in reality. Similarly, the

Initial Temperature τ_0 = 1948 degrees abs = 1675 degrees C

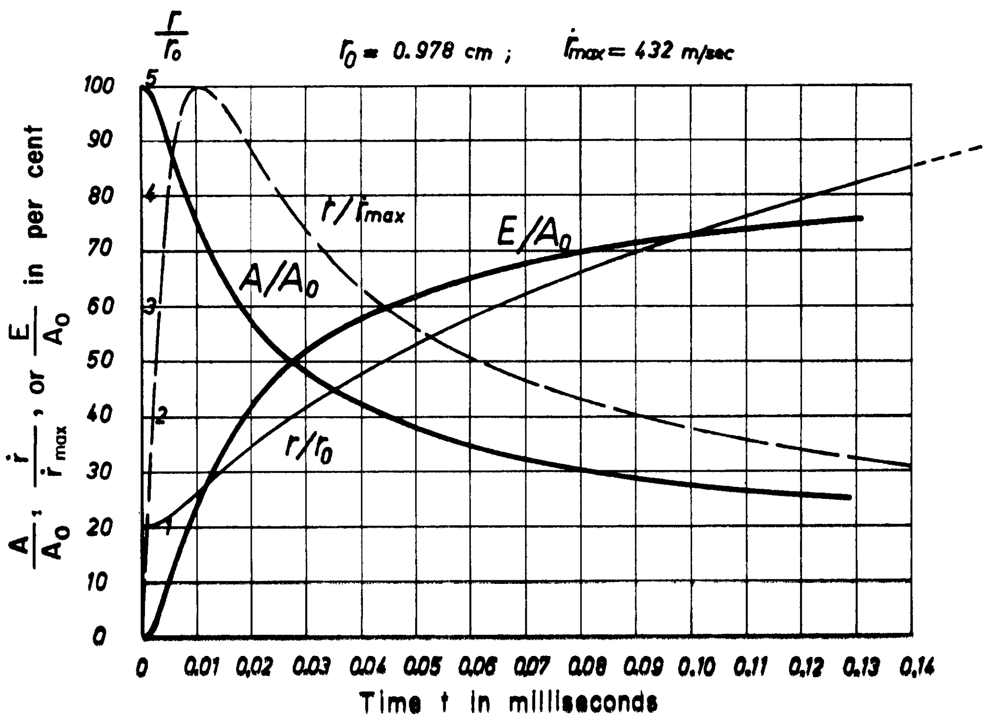

Figure 14a - First Oscillation

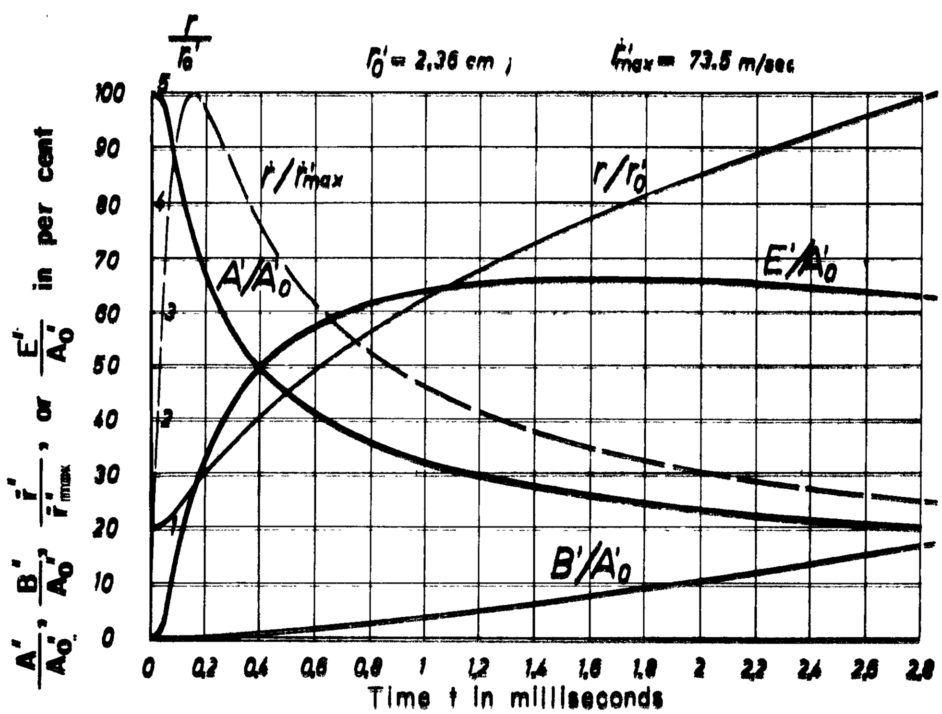

Figure 14b - Second Oscillation

Figure 14 - Initial Stage of Oscillation of the Gas Globe Produced by Detonating 5 + 1.2 Grams of TNT at a Charge Depth of 1 Meter

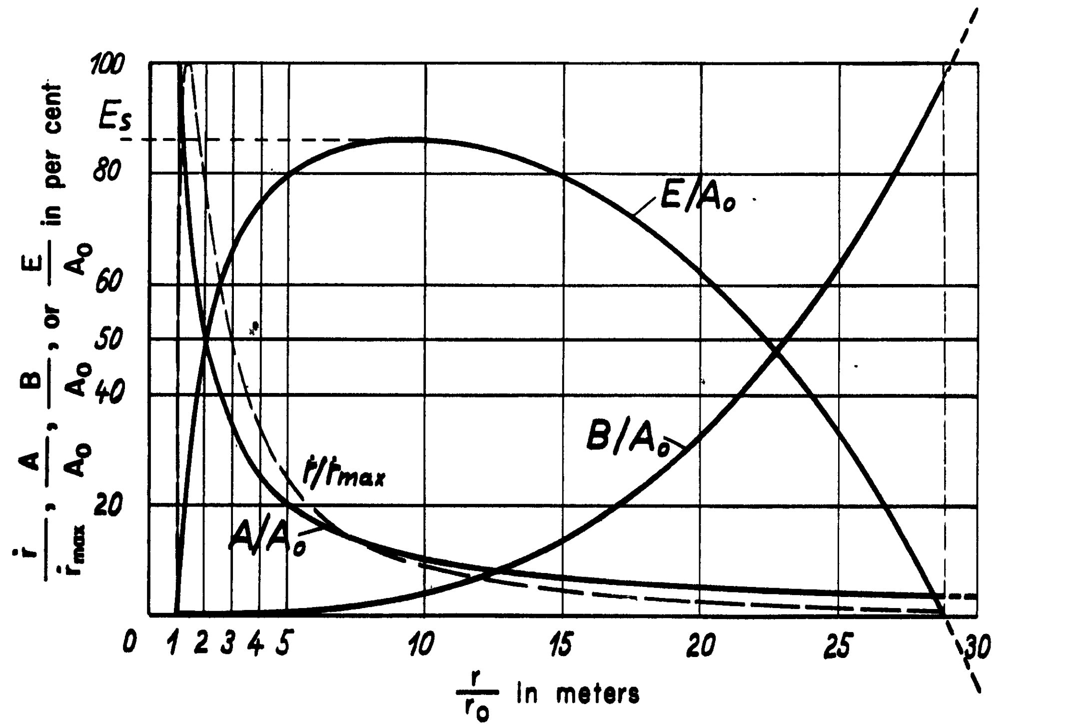

Figure 15a - First Oscillation

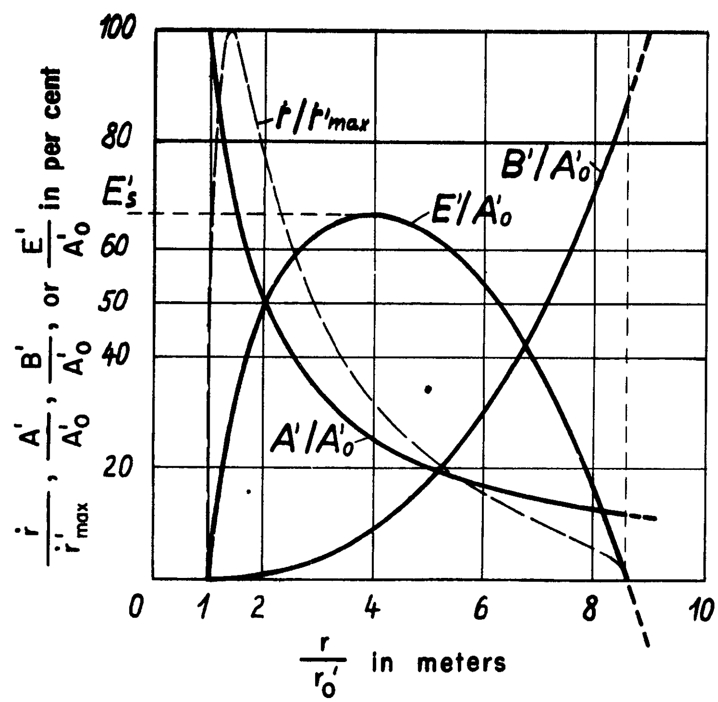

A Capacity for Work
B Displacement Work
E Kinetic Energy
r Gas Globe Radius
$\dot{r}$ Velocity of Expansion

Figure 15b - Second Oscillation

Figure 15 - Economy of Energy of the Gas Globe Produced by Detonating 5 + 1.2 Grams of TNT at a Charge Depth of 1 Meter

resulting from Equation [57], based on a specific gas volume v_G = 800 cm^3/gm, will be too low. The temperature and pressure curves at adiabatic change of state, as shown in Figure 16, are therefore not tenable in the initial state, as the pressure wave is not considered. The same holds true for the second minimum.

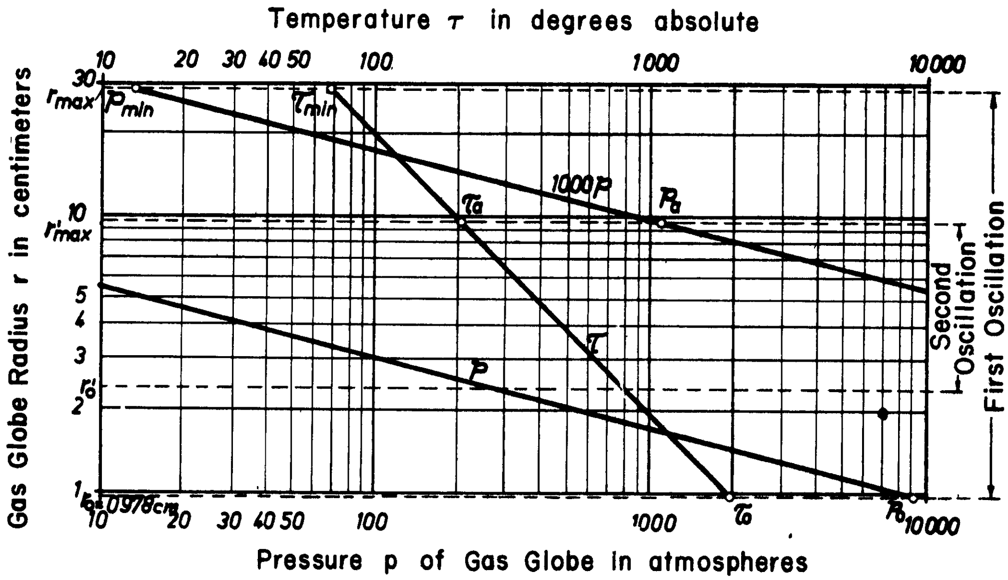

Figure 16 - Pressure and Temperature Curves for
Adiabatic Change of State of Gas Globe

The state of equalization, defined by $p = p_a$, sets in according to Equation [54] for

$$r_a = 9.31 \text{ cm}$$

$$\text{at } \tau_a = 205 \text{ degrees abs} = -68 \text{ degrees C}$$

In the state of maximum expansion, where $r = r_{max}$, pressure and temperature have dropped to

$$p_{min} = 0.0133 \text{ atm}; \quad \tau_{min} = 68 \text{ degrees abs} = -205 \text{ degrees C}$$

as can be read from Figure 16 or as calculated from the adiabatic equation.

b. SECOND OSCILLATION

In the investigation of the second oscillation all terms will be distinguished from those for the first oscillation by the prime sign; as a guiding concept, it will be assumed that the transition from the first oscillation to the second is adiabatic. Then the identical states of equalization $r_a' = r_a$, and $p_a' = p_a$ or $\tau_a' = \tau_a$ will prevail as in the first oscillation, and the curves derived in Section 9 (Figures 8 and 9) can be used. For measurements we take the

Period of Oscillation $T' = 0.0375$ second

which must be referred to the

Period of Sonic Oscillation $T_1 = 0.0281$ second

pertaining to the state of equalization r_a, p_a according to Equation [40] for the curve diagram, Figure 9. For $T'/T_1 = 1.334$, the

Expansion Factor $m' = 8.60$ and $\mu' = 1/m' = 0.1163$

can be read off. According to Equation [15'] or Figure 3,

$$\eta_r' = 1.041; \quad \alpha' = 0.1116; \quad \beta' = 1.037 \times 10^{-4}$$

pertain to the foregoing, supplying all the data necessary to permit treating the second oscillation as in Section a. However, the values of interest can also be read from Figure 8, as the state of equalization is already known at this time. Primarily, the

Maximum Radius of the Globe $r'_{max} = 20.35$ cm

is found in surprisingly good agreement with measurement; furthermore, we get the initial state

$$r_0' = 2.37 \text{ cm}, \; p_0' = 264 \text{ atmospheres}$$
$$\tau_0' = 805 \text{ degrees abs} = 532 \text{ degrees C}$$

which can also be found from Figure 16, as the pressure and temperature curves for both oscillations are the same, owing to the identity of the states of equalization. The real radius of the second minimum will lie between r_0 and r_0' and may be taken as 1.7 cm by taking the mean. This is therefore considerably below the apparent value of 10 cm obtained by measurement.

The curve of the oscillation plotted in Figure 13 agrees well with observation, except in the vicinity of the minima. Lamb's approximation shows graphic agreement to about $r = 5r_0'$ only, corresponding to the smaller expansion factor. The initial stage including the velocity curve for which $\dot{r}'_{max} =$ 53.5 m/sec is recorded in Figure 14.

Within the scope of this treatment, it must be assumed that the first oscillation reverts only as far as r_0', p_0', τ_0', and not to the initial state r_0, p_0, τ_0, and instead of achieving the original capacity for work A_0, it now attains $A_0' = 1.028$ kg-cal only. The excess is imparted to the second pressure wave and dissipated in additional energy losses.

15. BALANCE OF ENERGY

An energy balance for individual phenomena in underwater explosions will be of general interest. Therefore, the values already given will be summarized again and complemented by a few additional ones.

The evaluation in Section 14, based on high-speed photographs of underwater explosions with small charges, already permitted establishment of a certain energy balance. There it was shown that, of the total energy contained in the explosive, only 47.8 per cent was imparted to the first oscillation of the gas globe. Hence the remaining 52.2 per cent of the total energy will have to be assigned to the first pressure wave or to other energy losses. If the original energy of the explosive is set at 100 per cent, the following energy balance can be expressed:

Energy of the Explosive, 100 per cent

First Pressure Wave and Energy Losses Immediately after Detonation, 52.2 per cent

Total Energy of the First Oscillation, 47.8 per cent (Maximum Thrust Energy, 41 per cent)

Second Pressure Wave and Energy Losses in the Second Minimum, 28 per cent

Total Energy of the Second Oscillation, 19.8 per cent (Maximum Thrust Energy, 13 per cent)

A more accurate balance can be established on the basis of the measurements already cited with 100-gm charges of the explosive mixture consisting of 45 per cent TNT and 55 per cent RDX, because surface effects were eliminated by the charge depth. From these measurements (see Section 13) the constant $C_T = 0.3075$ follows directly, and therefrom the gas globe energy is found to be 42.85 kg-cal, while the energy content of 100 gm of explosive charge by measurements made on 5-gm charges in the explosive calorimeter was 99 kg-cal. Therefore, the first pressure wave and the simultaneous energy losses contain 57 per cent of the explosive energy.

Energy of the Explosive, 100 per cent

First Pressure Wave and Energy Losses Immediately after Detonation, 57 per cent

Total Energy of the First Oscillation, 43 per cent (Maximum Thrust Energy, approximately 37 per cent)

In comparing the two energy balances, it must not be forgotten that the first balance was arranged for TNT and the second for the mixture composed of 45 per cent TNT and 55 per cent RDX.

In general, it can be said on the basis of the conditions just outlined that the first oscillation contains a little less than half the explosive energy measured calorimetrically. The total energy of the second oscillation is again a little less than half of the total energy of the first oscillation.

16. MEASUREMENT OF IMPACT TIMES

As described earlier in this report, during the oscillation of the gas globe pressure waves radiate at the individual minima. These successive waves, particularly with large charges, follow each other at increasing intervals. They are often clearly audible and are perceived as impacts. Thus the term "measurement of impact times" (Stosszeitmessung) has become current for the measurement of the period of oscillation of the gas globe.

The actual significance of the measurement of impact times is based on the relation between the gas globe energy A_0 and the period of oscillation T, given by Equations [1] and [22]. For water, where $\gamma = 1$,

$$T \approx 0.0011458\sqrt{\gamma'}\sqrt[3]{\frac{L}{p_a^{2.5}}}\sqrt[3]{\frac{p_0}{(\kappa - 1)s'}} = \frac{0.0011458}{p_a^{5/6}}\sqrt[3]{\underbrace{\frac{V_0 p_0}{\kappa - 1}}_{A_0}}$$

For sea water, about 1 per cent must be added. Therefore, when T is measured in seconds and p_a in atmospheres, it follows that

$$A_0 \approx 15{,}570\, p_a^{2.5} T^3 \text{ kg-cal} \qquad [60]$$

The gas globe energies A_0 of two charges detonated at the same depth vary approximately as the cubes of the impact times T. As the latter can be measured by means of underwater microphones, the measurement of impact times is a convenient criterion for evaluating the energy of explosives.

The significance of the measurement of impact times for determination of the gas globe energy is augmented by the fact that the relationship for the impact time, Equation [22], is accurate even in second approximation and was verified experimentally with surprising accuracy; see Section 13. Furthermore, as already emphasized, we may add that for identical detonations under constant conditions the impact times can be reproduced very accurately.

These considerations show that the best method to ascertain the gas globe energy is measurement of the "impact time." Therefore, determination of the impact time can be developed into a direct measuring method. To apply this method of measurement in practice, the following essential points should be emphasized.

"Regulation charges" of identical weights must be detonated and the impact time must be picked up with the aid of a microphone and recorded by an oscillograph. In Figure 17, such an oscillogram is shown. Precautions must be taken to maintain constant charge depth and precisely uniform quantities of explosive charge in these measurements. Despite maintenance of constant charge depth, the impact times may still fluctuate owing to variation of the air pressure which affects the total pressure p_a at the point of detonation.

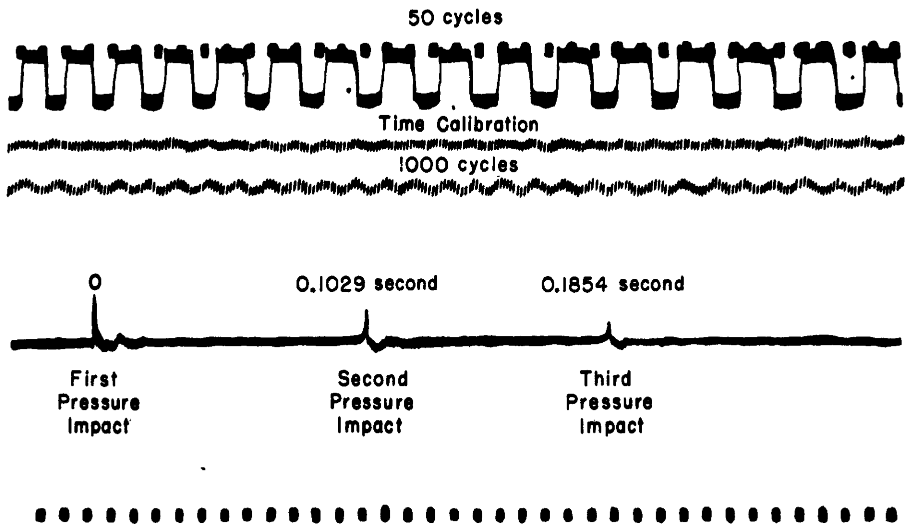

Figure 17 - Diagram of Impact-Time Measurement in Underwater Explosions

These fluctuations, however, can be eliminated practically by using Equation [22] judiciously. The measured impact times are usually reduced to normal air pressure.

Among the numerous possible applications of the measurement of impact times, the following are mentioned briefly:

a. With the method of measurement of impact times, a simple and rapid comparison of the energy of various explosives is possible for conditions which correspond extensively or entirely to those encountered in practice, that is, for detonation of explosives below the surface of the earth or under water.

b. From the fact that the measurement of impact times is in final analysis a measurement of energy, another important application exists. In general, for explosives which are difficult to detonate or for materials whose explosive character is doubtful at best, quantitative data on the initiation of complete or partial detonation or the extent of induced detonation can hardly be given. Here the measurement of impact times permits quantitative statements by a simple method.

c. When the quantity and type of an explosive are known, the charge depth can be ascertained immediately by Equation [30]. This method was used, for example, to determine the depth of detonation of depth charges.

17. GAS GLOBE ENERGY AS A CHARACTERISTIC QUANTITY FOR EXPLOSIVES

The theoretical explanation of the physical phenomena attendant upon detonation of an explosive in water led automatically to a characteristic quantity for each explosive, the gas globe energy.

It must be emphasized that, when measuring this quantity by the impact-time method, maintenance of constant test conditions is very simple because the detonations always occur in water. In all other comparisons of effectiveness, such as measurement of effectiveness in a lead block by Trauzl (lead-block expansion) or measurement of the funnel-shaped hole in the ground in underground explosions (crater effect), for example, rigorously constant test conditions can be maintained only by virtue of considerably greater expense and equipment; even then, such constant test conditions cannot be attained in most cases.

The significance of the gas globe energy A_0, introduced as a characteristic quantity, is already evident from the fact that the maximum kinetic energy E_S, imparted to the water at detonation, is approximately equal to it. However, a basic deficiency is entailed. Owing to the simplifying assumption of incompressible water used in the theory herein outlined previously, the radiated pressure wave did not appear in the test results. Fundamentally, therefore, the gas globe energy still does not furnish an absolute, flawless characteristic for an explosive.

In contrast to the only other possible method of measuring the energy produced at detonation, measurement in the explosive calorimeter, determination of the gas globe energy by means of the impact-time method offers decided advantages. In the calorimeter, only the heat of reaction can be measured during reactions involving minimum quantities of explosives. Such quantities reach their maximum at 10 gm. The type of the reaction of explosives, i.e., detonation or explosive combustion, especially the less sensitive explosive mixtures, is often just as uncertain as the completely unknown secondary reactions of the products of combustion during the considerably protracted period of thermal equalization occurring in the calorimeter. The gas globe energy, and therefore the work capacity of an explosive, in contrast, can be measured without great effort by the impact-time method, even for charges of greatest size. In fact, such measurement can be made under conditions similar, or even identical, to full scale.

The points herein described, in themselves, permit recognition of the gas globe energy as a basic quantity in the study of explosives. Accurate investigation of the underwater explosive effect shows beyond this that it is one of the most basic characteristics for an underwater explosive, and it can probably be added that it is the most important characteristic quantity with respect to destruction of ships. Investigation of the effects of underwater explosions on ships show that at a greater distance from the target, the pressure wave only is effective. In such a case, truly serious damage is exceptional. Lethal damage to a ship, such as blasting holes in the ship's shell or demolition of torpedo bulkhead structures below the waterline, occurs only if the point of detonation is so close that the hull is within the zone occupied by the gas globe. It has been proved experimentally that the gas globe energy is principally responsible for such types of demolition.

However, this proves that the gas globe energy determined by the impact-time method is one of the most essential characteristic quantities for underwater explosives.

On the basis of these facts, the gas globe energy derived from theory can therefore be designated as an important characteristic for explosives in general and probably the most important for underwater explosives in particular.

18. SUMMARY

The problem of expansion of the products of combustion in underwater explosions has been treated theoretically. The expression for the adiabatic expansion of the gas globe in undisturbed, incompressible water was rigorously evaluated. Special assumptions with respect to κ, introduced as a constant only, were largely avoided. The exact equations for the maximum gas globe radius, Equation [18], and the period of oscillation, Equation [30], are

$$r_{\max} = \frac{C_r}{\eta_r} \sqrt[3]{\frac{L}{p_a}} \quad \text{and} \quad T = C_T \eta_T \sqrt[3]{\frac{L}{p_a{}^{2.5}}} \sqrt{\gamma'}$$

where C_r and C_T are constants of the explosive and where the correction factors η_r and η_T, which are functions of depth, approach unity. Their respective values can be seen in Figures 3 and 4. We find that η_r as a function of depth is a small magnitude of first order, whereas η_T is even smaller, being merely of second order.

The curve of the oscillation of the gas globe is determined by a trigonometric substitution described in Section 6. For large values of the expansion factor m, a convenient development in a series was given. Comparison with Lamb's approximation $p_a = 0$ shows its applicability over a considerable range about the minimum; see Section 7. For the limiting case where $m = 1$, the sonic oscillation of the globe was found; see Section 8.

Comparison of various stages of oscillation of the same gas globe proved useful for theoretical comprehension of its pulsating oscillations, later damped by energy losses in underwater explosions. These phenomena were comprehended for the first time in this way in this treatise.

The most important magnitudes were generally formulated and plotted as curves, to facilitate application to any given numerical example with minimum effort.

The equations derived for the maximum radius and period of oscillation of the gas globe were checked for their reciprocal functional relationship, as well as individually by means of the measurements made; see Section 13. Agreement between theory and experiment was good, and for the impact time specifically, excellent. This agreement between theory and experiment was further checked for the total curve for detonation of a charge of 5 + 1.2 gm of TNT at 1 m below the surface of the water and was found to be very good; see Section 14. However, it was found that the minima must be much more sharply defined than was apparent from former measurements. The pressure and temperature curves, based on adiabatic change of state, and the duration of the energy as well were calculated completely and represented graphically for the given example.

The energy balance for underwater explosions was established and discussed in terms of various measured data; see Section 15.

The importance of the measurement of impact times for the determination of the gas globe energy was exhaustively discussed in Section 16, and a number of problems were proposed whose mathematical treatment was either facilitated or actually made possible at all by measurement of impact times.

The special significance of the gas globe energy, determined easily with the aid of the measurement of impact times especially for the evaluation of underwater explosives, was emphasized; see Section 17.

REFERENCES

(1) "The Early Stages of a Submarine Explosion," by H. Lamb, Philosophical Magazine, Vol. 45, 1923, pp. 257-265.

(2) "On Musical Air-Bubbles and the Sounds of Running Water," by M. Minnaert, Philosophical Magazine, Vol. 16, 1935, pp. 235-248.

(3) "Adiabatisch pulsierende Gaskugel in unendlich ausgedehnter kompressibler Flüssigkeit" (Adiabatically Pulsating Gas Globe in a Compressible Liquid of Infinite Extent), by K. Zoller, Forschungsanstalt Graf Zeppelin Report 221, 1942.

(4) "Die Schwingungen der bei einer Unterwassersprengung entstehenden Gasblase und die Druckverteilung in ihrer Umgebung" (Oscillations of a Gas Globe in an Underwater Explosion and the Pressure Distribution in Its Vicinity), by W. Döring, ZWB Report 1818, 1943.

(5) "Die Schwingung der Schwadenkugel bei einer Unterwassersprengung" (Oscillation of the Gas Globe Formed by the Products of Combustion in an Underwater Explosion), by Gerhartz, ZWB Report 1996.

(6) "Adiabatisch pulsierende Gaskugel in unendlich ausgedehnter Flüssigkeit" (Adiabatically Pulsating Gas Globe in a Liquid of Infinite Extent), by K. Zoller, Forschungsanstalt Graf Zeppelin Report 166.

(7) "Die Massenbewegung des Wassers bei Unterwasser Explosionen" (Mass Movement of Water in Underwater Explosions), by C. Ramsauer, Annalen der Physik, Vol. 72, 1923, pp. 265-284.

PBNC-3290-10-15-47-125